

**Resonance-enhanced multiphoton ionization (REMPI) spectroscopy of bromobenzene and its perdeuterated isotopologue: assignment of the vibrations of the  $S_0$ ,  $S_1$  and  $D_0^+$  states of bromobenzene and the  $S_0$  and  $D_0^+$  states of iodobenzene**

Anna Andrejeva, William D. Tuttle, Joe P. Harris, and Timothy G. Wright<sup>a</sup>

School of Chemistry, University of Nottingham, University Park,  
Nottingham NG7 2RD, UK

<sup>a</sup> Corresponding author. Email: Tim.Wright@nottingham.ac.uk

**Abstract**

We report vibrationally-resolved spectra of the  $S_1 \leftarrow S_0$  transition of bromobenzene using resonance-enhanced multiphoton ionization (REMPI) spectroscopy. We study bromobenzene- $h_5$  as well as its perdeuterated isotopologue, bromobenzene- $d_5$ . The form of the vibrational modes between the isotopologues and also between the  $S_0$  and  $S_1$  electronic states are discussed for each species, allowing assignment of the bands to be achieved and the activity between states and isotopologues to be established. Vibrational bands are assigned utilizing quantum chemical calculations, previous experimental results and isotopic shifts. Previous work and assignments of the  $S_1$  spectra are discussed. Additionally, the vibrations in the ground state cation,  $D_0^+$ , are considered, since these have also been used by previous workers in assigning the excited neutral state spectra. We also examine the vibrations of iodobenzene in the  $S_0$  and  $D_0^+$  states and comment on previous assignments of these. In summary, we have been able to assign corresponding vibrations across the whole monohalobenzene series of molecules, in the  $S_0$ ,  $S_1$  and  $D_0^+$  states, gaining insight into vibrational activity and vibrational couplings.

## I. INTRODUCTION

The present work is a continuation of our previous work on fluorobenzene<sup>1</sup> and chlorobenzene,<sup>2</sup> in each case including the perdeuterated isotopologue. In those studies we recorded one-colour (1+1) resonance-enhanced multiphoton ionization (REMPI) spectra from 0–3000 cm<sup>-1</sup> and assigned the vibrational structure observed. The spectra showed rich structure from both Franck-Condon allowed  $a_1$  and vibronically-allowed  $b_2$  vibrations, with higher-wavenumber features mainly consisting of overtones and combinations of vibrations seen to lower wavenumber. (Here, we position the molecule in the  $yz$  plane, to establish the  $b_1/b_2$  labels unambiguously.) There were numerous Fermi resonances (FRs) observed, with these generally being different between the respective isotopologues, owing to vibrations moving in and out of resonance because of isotopic shifts. In the case of chlorobenzene, shifts arising from the presence of both <sup>35</sup>Cl and <sup>37</sup>Cl were extremely useful in establishing the assignment when there was more than one possibility. In the present work we shall denote the isotopologue of perhydrogenated bromobenzene as BrBz- $h_5$  and similarly for the fully-deuterated isotopologue, BrBz- $d_5$ ; we will only note the isotope of Br as required, but only little use is made of <sup>79</sup>Br/<sup>81</sup>Br shifts in this work, as these were so small. When required, the other monohalogenated benzenes will be denoted in a similar manner, using FBz for fluorobenzene, ClBz for chlorobenzene and IBz for iodobenzene. We concentrate initially on BrBz and then at the end of this paper we shall briefly discuss IBz.

The infrared (IR) and Raman spectra of BrBz- $h_5$  have been reported by a number of workers,<sup>3,4,5,6,7</sup> with reasonable consistency between the reported values where these have been observed in more than one study. The assignment of the spectra has been achieved in terms of symmetry, by noting the band-type, and also in terms of expected positions of vibrations based upon various mass-scaling rules. Two main schemes for labelling the vibrations have been employed, with Wilson<sup>8</sup>-type labels being used by Varsányi<sup>5</sup> and, albeit with some (unexplained) switches, by Walter et al.<sup>9</sup> As noted and discussed in our previous work<sup>10</sup> the Varsányi (Wilson) labels are used inconsistently across the monohalobenzenes and so we use a different labelling scheme based on the Mulliken<sup>11</sup> labelling of the FBz  $S_0$  modes, and we denote these  $M_i$ , with the motions available in ref. 10. This scheme maintains the same label for the same vibrational motion, and hence vibrational activity can be easily compared between molecules. (It should be noted that using the Mulliken labelling for the heavier monosubstituted halobenzenes will give some vibrations in a different order, owing to different mass shifts – see ref. 10.)

Very brief reports of the UV absorption spectrum of bromobenzene vapour have been given by Walerstein<sup>12</sup> and Sreeramamurty.<sup>13</sup> In addition, a study by Prakash and Singh<sup>14</sup> has reported a reasonably detailed UV absorption spectrum of BrBz vapour, predominantly at 0 °C. Klimusheva et al.<sup>15</sup> have reported absorption spectra of bromobenzene in both vapour (20 K) and crystals (4 K), but little experimental detail is given, nor are any spectra shown. We shall comment on these studies at appropriate points below.

Jet-cooled studies of the  $S_1 \leftarrow S_0$  transition has been reported by Dietz et al.<sup>16</sup> and Boesl and coworkers<sup>9,17</sup> where Wilson/Varsányi labelling was employed. The Wilson/Varsányi assignments between the two main studies<sup>9,16</sup> were not wholly consistent, and in part this results from the fact that many of these do not correspond to the correct vibrational motion. Such assignments can be made by analogy with spectra from similar molecules and a detailed consideration of mass and electronic shifts; however, the most robust assignment will come from comparison also with reliable quantum chemical calculations. In the below we shall discuss the previous assignments with those here. We shall establish assignments of the observed bands that are consistent with our previous monohalobenzene work, and so remove the ambiguity of the previous assignments for bromobenzene and provide a more coherent picture of the vibrational activity in the monohalobenzene species.

The vibrations of the cation have been probed via conventional photoelectron spectroscopy (PES),<sup>18, 19</sup> REMPI-PES<sup>9</sup> and one-photon MATI studies.<sup>20</sup> In the case of the REMPI-PES experiments, the assignment of the photoelectron spectrum and the resonant  $S_1$  level are linked, and so these will be discussed as part of the present work in Section IV. C. 4

BrBz- $d_5$  has been much less studied compared to its non-deuterated isotopologue. Vibrationally-resolved IR and Raman spectra of the  $S_0$  state have been reported by Nanney et al.,<sup>21</sup> where assignments were given in Mulliken notation and (cautiously) in terms of an approximate description of the atomic motions; comparison was also made to the wavenumbers of the corresponding vibrations in ClBz- $d_5$  and FBz- $d_5$ . The BrBz- $d_5$  vibrations were given Wilson-type labels by Varsányi<sup>5</sup> (see Table 1). To the best of our knowledge there have been no reports of the  $S_1 \leftarrow S_0$  transition or any photoelectron spectrum for this isotopologue.

In the present work, we employ one-colour REMPI spectroscopy to record rotationally-cold, vibrationally-resolved electronic spectra of the  $S_1 \leftarrow S_0$  transition in BrBz- $h_5$  and BrBz- $d_5$ , for each of their <sup>79</sup>Br and <sup>81</sup>Br isotopologues. The spectra are assigned using: the observed experimental isotopic shifts; available previous experimental and theoretical results; and quantum chemical calculations for all of the isotopologues, carried out in the present work. The REMPI spectrum of BrBz- $d_5$  is reported here for the first time and, as with our previous work on FBz and ClBz,<sup>1,2</sup> we examine how the vibrations in the perdeuterated isotopologue compare to those of the perhydrogenated molecule. In addition, we consider the Duschinsky mixing of the vibrational modes that occurs between the  $S_0$  and  $S_1$  states for each isotopologue. In some cases, comparison between the activity seen in BrBz with that seen in FBz and ClBz is insightful. Since some of the assignments of the  $S_1$  state vibrations depend on those of the cation via REMPI-PES spectra, we shall also examine the vibrations of the ground state cation of BrBz.

Towards the end of the paper, we shall also consider the vibrations of the  $S_0$  state of IBz. We shall not consider the  $S_1$  state vibrations, as this state is known to be extremely short lived and no fluorescence or REMPI spectrum has been reported (see later). We shall also consider the vibrations of the ground state cation, since

these have been observed by direct photoionization both using conventional PES<sup>19, 22</sup> and also mass-analyzed threshold ionization (MATI) spectroscopy.<sup>20</sup>

## II. EXPERIMENT

The third harmonic (355 nm) of a neodymium-doped yttrium aluminium garnet laser (Nd:YAG, Surelite III, 10 Hz) was used to pump a tuneable dye laser (Sirah Cobra Stretch), operating on Coumarin 503. The fundamental output of the dye laser was frequency doubled by a beta-barium borate (BBO) crystal in order to obtain tuneable UV radiation across the wavenumber region of interest.

BrBz-*h*<sub>5</sub> (Aldrich, 99.8% purity) or BrBz-*d*<sub>5</sub> (Aldrich, 99 atom% D) vapour, each with the naturally-occurring ratio of <sup>79</sup>Br:<sup>81</sup>Br, was seeded in ~5 bar of helium carrier gas and the gaseous mixture was passed through a General Valve pulsed nozzle (750 μm, 10 Hz, opening time of 180 μs) to create a free jet expansion. In our previous work on FBz and ClBz we employed Ar as the seeding gas, but we found the BrBz spectra were too warm (and hence broad) when this was used here; we attribute this to clustering and subsequent break-up; this also occurred even when using Ne. On the other hand, using He, we found it much easier to obtain cold spectra. The focused, frequency-doubled output of the dye laser passed through a vacuum chamber where it perpendicularly intersected the free jet expansion between two biased electrical grids located in the extraction region of a time-of-flight spectrometer. After (1+1) ionization occurred, the resulting ions were extracted and detected by a dual microchannel plate (MCP) detector. The signal was passed to an oscilloscope (LeCroy LT342 Waverunner) for monitoring, and a boxcar (SRS SR250) for integration and averaging; the averaged signal was then relayed to a computer for storage and analysis. The timing of the laser pulse relative to the opening time of the pulsed nozzle was controlled using a digital delay generator. The delays were varied to produce optimum conditions to ensure that the coldest part of the beam was probed. The calibration procedure is described in Section IV.

## III. COMPUTATIONAL METHODOLOGY

In order to aid in the assignment of the spectra, the vibrational frequencies of each molecule were calculated using the GAUSSIAN 09 software package.<sup>23</sup> For the S<sub>0</sub> ( $\tilde{X}^1A_1$ ) state and the ground cation D<sub>0</sub><sup>+</sup> ( $\tilde{X}^2B_1$ ) state, (U)B3LYP/aug-cc-pVTZ calculations were used; whereas for the S<sub>1</sub> ( $\tilde{A}^1B_2$ ) state TD-B3LYP/aug-cc-pVTZ calculations were employed; for Br and I, these were the valence forms of these basis sets, used with the ECP10MDF and ECP28MDF small-core, relativistic effective core potentials. All of the harmonic vibrational wavenumbers were scaled by the widely used factor of 0.97, although this is only an approximate way of getting “anharmonic” values. For the unrestricted calculations  $\langle S^2 \rangle$  values were all ~ 0.76 showing that spin contamination was minimal.

The vibrational modes of the BrBz-*h*<sub>5</sub> and IBz-*h*<sub>5</sub> S<sub>0</sub> states were labelled by comparing the molecular vibrational displacements with those of FBz-*h*<sub>5</sub> via a generalised Duschinsky matrix approach employing the FC-LabII program,<sup>24</sup> as discussed in ref. 10. This provided a clear assignment of the phenyl ring-localized vibrations. For BrBz-*d*<sub>5</sub> and IBz-*d*<sub>5</sub>, the molecular vibrational motions were compared to those of BrBz-*h*<sub>5</sub> and IBz-*h*<sub>5</sub>, respectively, in their S<sub>0</sub> states via a generalized Duschinsky approach using FC-LabII. Similarly, vibrations in the S<sub>1</sub> and D<sub>0</sub><sup>+</sup> states could be compared to those of the respective S<sub>0</sub> state, and those of the respective S<sub>1</sub> and D<sub>0</sub><sup>+</sup> states to each other.

## IV. RESULTS AND ASSIGNMENTS

### A. Overview of the S<sub>1</sub>←S<sub>0</sub> spectra.

The (1+1) REMPI spectra of BrBz-*h*<sub>5</sub> (upright, top trace) and BrBz-*d*<sub>5</sub> (inverted, bottom trace) from 0 – 3050 cm<sup>-1</sup> are shown in Figure 1 — the assignments are discussed below. Only the spectra for the <sup>79</sup>Br isotopologues are shown; the spectra of the <sup>81</sup>BrBz isotopologues exhibited only very small isotopic shifts compared to the <sup>79</sup>BrBz isotopologues, and will only be commented on occasionally. We have not corrected for laser intensity, as we believe this is not straightforward to do reliably.

We calibrate the <sup>79</sup>BrBz-*h*<sub>5</sub> spectrum to the band origin of 36991.5 ± 0.2 cm<sup>-1</sup> by comparing with a simulation of the origin band origin using PGOPHER<sup>25</sup> and using the rotational constants taken from Ref. 26; additionally, this allowed a rotational temperature of 20–30 K to be established: warmer than we obtained for FBz and ClBz, but in line with the use of He rather than Ar. It was then found that the <sup>81</sup>BrBz-*h*<sub>5</sub> origin band was at the same position, within our experimental uncertainty, showing that the S<sub>1</sub> origin bands of the <sup>79</sup>Br and the <sup>81</sup>Br isotopologues are within 0.5 cm<sup>-1</sup> of each other, consistent with the result of de la Cruz et al.,<sup>27</sup> who determined the difference to be < 0.02 cm<sup>-1</sup>. For the BrBz-*d*<sub>5</sub> origin transition, an isotopic blue shift of 171.4 cm<sup>-1</sup> is determined from our spectra, which locates the origin at 37162.9 ± 0.5 cm<sup>-1</sup>. The two spectra presented in Figure 1 have been plotted on a relative scale, with the origin transitions each shifted to zero for straightforward comparison between the different isotopologues. Our vibrational bands are not fully rotationally resolved in either the BrBz-*h*<sub>5</sub> or BrBz-*d*<sub>5</sub> spectra and so we have employed the wavenumber of the most intense part of each vibrational band, in order to determine consistent vibrational spacings; although this may give small discrepancies with respect to the actual vibrational band origins, this is acknowledged to be the most consistent way of reporting these spacings. In any case, we have ascertained the reliability of this procedure by simulating different band profiles and comparing the position of the maxima in the rotational envelope relative to the band center. We find that these positions fall within the stepsize of our scans (0.5 cm<sup>-1</sup>) and so any discrepancy in vibrational spacing arising from different band types will not introduce an error of more than 1 cm<sup>-1</sup>; this will be similar to the error that would have been obtained employing band centers to derive the vibrational spacings.

We have checked our calibration against other spectra and although there are discrepancies, it does not seem that there are “bigger errors” to higher energy; we have checked our spectra in both wavenumber

and wavelength, and against spectra of other molecules, and our calibration appears to be sound across the spectral range cited.

The BrBz- $h_5$ / BrBz- $d_5$  isotopic shift of each vibration is clearly mode specific as participation of the hydrogen atoms is different – this will be more clearly seen in expanded spectral views presented later. The  $^{79/81}\text{Br}$  isotopic shift is very small,  $< 1 \text{ cm}^{-1}$  for 29 of the 30 vibrational modes, apart from for  $M_{11}$ , which has an isotopic shift of  $1.6 \text{ cm}^{-1}$  for BrBz- $h_5$  and BrBz- $d_5$  isotopologues. (For the interested reader, calculated vibrational wavenumbers of the  $S_0$ ,  $S_1$  and  $D_0^+$  states of  $^{81}\text{BrBz-}h_5^{(+)}$  and  $^{81}\text{BrBz-}d_5^{(+)}$  are given in Tables S1 and S2 of the Supplementary Material.<sup>28</sup>)

In the following, we shall tackle the assignments of the BrBz- $h_5$  and BrBz- $d_5$  spectra simultaneously, considering spectral ranges separately. Our assignments are aided by previous work on BrBz- $h_5$  as well as the calculated vibrational frequencies, and use will also be made of previously-observed activity in our corresponding spectra of FBz and ClBz.<sup>1,2</sup> First we shall comment on the vibrational assignments of the  $S_0$  state.

## B. Calculated vibrational wavenumbers.

### 1. $S_0$ state

We shall only discuss vibrations for the  $^{79}\text{Br}$  isotopologues here – those for the  $^{81}\text{Br}$  one are very similar, and the calculated values are given as supplementary material.<sup>28</sup>

In ref. 10 we briefly discussed and assigned the  $S_0$  vibrations of BrBz- $h_5$  in terms of the  $M_i$  vibrational modes; as such, we shall only note that the motions are very different to those of benzene, and so Wilson modes are inappropriate (Table 1 shows how mixed some of the modes are). On the other hand, correspondences between the vibrations of FBz- $h_5$  and BrBz- $h_5$  are very good (see Table 1 and Figure 2). As a consequence, we provide the Wilson/Varsányi mode labels used by other workers in Table 1, but only to aid the reader. In the text here we shall use  $M_i$  labels, when discussing our assignment and also when comparing to previous work. In Table 2 we compare our calculated vibrational wavenumbers for BrBz- $h_5$  with the experimental ones, where excellent agreement is seen. (We note that our calculated values are in very good agreement with the B3LYP/aug-cc-pVDZ values given in ref. 10, bearing in mind those were unscaled, as are the comparisons with the Wilson modes of benzene.)

For BrBz- $d_5$  we note that Nanney et al.<sup>21</sup> reported IR and Raman spectra, assigning the modes by virtue of the rotational band type and by comparison with vibrational wavenumbers for FBz- $d_5$  and ClBz- $d_5$ ; these trends were continued when assigning the corresponding spectra of IBz- $d_5$ , which will be mentioned later. Wavenumbers for all 30 vibrational modes were obtained from fundamentals, overtones and combination bands, although a couple were uncertain. The assignment was given in terms of Mulliken nomenclature, and as noted

above this could lead to some discrepancies with the  $M_i$  labels owing to reordering following mass-dependent shifts across the monohalogenated benzene series. Since the agreement between the calculated and experimental values is excellent for both BrBz- $h_5$  and BrBz- $d_5$ , then we can use the calculated values to confirm the assignment of Nanney et al.'s wavenumber values<sup>21</sup> to the  $M_i^d$  labels. (We note that while the appending of the  $d$  superscript to the  $M_i$  labels is often superfluous, it is maintained for consistency and clarity both within the present text, and with our earlier work.) The Duschinsky matrix in Figure 3 shows that the motions of the  $M_i^d$  vibrations are very similar to the  $M_i$  modes in most cases; however, the wavenumber ordering of the vibrations changes, as it does for FBz<sup>1</sup> and ClBz.<sup>2</sup> In particular, for FBz- $h_5$  the ordering is  $M_9 < M_8 < M_7 < M_6$  (by construction), while for FBz- $d_5$  the ordering is  $M_8^d < M_7^d < M_9^d < M_6^d$ ; for ClBz- $h_5$  the ordering is  $M_9 < M_8 < M_6 < M_7$ , while for ClBz- $d_5$  the ordering is again  $M_8^d < M_7^d < M_9^d < M_6^d$ . For BrBz, we find the same orderings in the  $S_0$  states as for the respective ClBz isotopologues. The assignment from Nanney et al.'s wavenumber values is straightforward in most cases; we merely note that the estimated 2275  $\text{cm}^{-1}$  value is consistent with our calculated value of 2269  $\text{cm}^{-1}$  for  $M_3^d$ , the wavenumber of  $M_8^d$  is uncertain since in ref. 21 a band at 817  $\text{cm}^{-1}$  was observed in the IR spectrum, but one at 826  $\text{cm}^{-1}$  observed in the Raman one; these are close enough to our calculated value of 815  $\text{cm}^{-1}$  that it is difficult to decide between them definitively.

## 2. $S_1$ state

The calculated wavenumbers for the  $S_1$  state of the  $^{79}\text{BrBz-}h_5$  and  $^{79}\text{BrBz-}d_5$  are given in Table 3; these have been used to help in the assignment of the spectra, together with previously reported assignments of the  $^{79}\text{BrBz-}h_5$  spectra. Figure 4 shows the Duschinsky matrices for the  $S_1$  vibrations in terms of the  $S_0$  ones for each isotopologue. As was the case for FBz and ClBz, these indicate that there is more rotation of the vibrational coordinates for BrBz- $h_5$  than for BrBz- $d_5$ , as such some of the vibrations in that  $S_1$  state will be somewhat different to those in the  $S_0$  state. In particular, we found that the  $M_8$  and  $M_9$  modes were significantly mixed (as we noted for ClBz), and have labelled these to be consistent with our previous work.

One other point of note is that in the Duschinsky matrix, the  $M_6^d$  and  $M_8^d$  modes are quite mixed in the  $S_0$  state, with the coefficients suggesting their order has changed; however, it is clear from the spectra here and our previous assignments of these modes for FBz and ClBz, that in fact the  $M_8^d$  vibration has the lower wavenumber. (It is then clear from the  $S_1 \leftarrow S_0$  Duschinsky matrix in Fig. 4b that the same ordering applies to the  $S_1$  state.) We think this anomaly lies in the similarity of these two modes (see ref. 10), with the major difference being the stretching of the carbon–substituent bond. As the substituent gets heavier, this motion becomes smaller, and then determining the difference between these two modes in the Duschinsky procedure becomes less clear although these can be identified visually in animations. The comparison of the  $-h_5$  and  $-d_5$  spectra with the corresponding ones for FBz and ClBz does, however, make the assignment of these modes clear, as noted above and discussed below.

## C. Assignment

We now move onto the assignment of the spectra, which we split into three main wavenumber regions. We shall discuss the assignment of the spectra for the  $^{79}\text{BrBz-}h_5$  and  $^{79}\text{BrBz-}d_5$ , with the assignments for the  $^{81}\text{Br}$  ones being the same. To assign the spectra, we have used the previous assignments as a guide, but have mainly relied on our calculated wavenumbers and our previous assignments of the  $\text{FBz}^1$  and  $\text{ClBz}^2$  spectra for both  $-h_5$  and  $-d_5$  variants. As low-wavenumber bands become assigned, the vibrational wavenumbers of these are used to assign the higher-wavenumber features; occasionally this process worked in reverse. We denote transitions by the upper vibrational level, since all transitions, unless noted, are from the zero point vibrational level in the ground electronic state.

### 1. Low wavenumber range (0- 750 $\text{cm}^{-1}$ )

#### a. $\text{BrBz-}h_5$

As may be seen from Figure 5, this region is dominated by the origin transition and that to the  $M_{29}$  level for both isotopologues. Concentrating first on  $\text{BrBz-}h_5$ , in the low-wavenumber region below  $300\text{ cm}^{-1}$  we see a similar pattern of features we saw previously for  $\text{FBz}$  and  $\text{ClBz}$ , and so these mostly can be straightforwardly assigned as shown in Figure 5 and Table 4. We note that the  $M_{11}$  band is slightly red shifted in the  $^{81}\text{BrBz-}h_5$  spectrum (not shown), and indeed this is a signature that helps in the assignment of higher wavenumber combination bands. It is a peculiarity of the monohalobenzenes that the calculated wavenumber for the  $M_{14}$  vibration in the  $S_1$  state is always in very poor agreement with the experimental value using the TD-B3LYP approach; indeed, in the present case, we did not even obtain a real value. As a consequence, we have relied on previous assignments and a process of elimination to assign features involving this vibration. First we note that at  $462\text{ cm}^{-1}$ , we find a band whose assignment to the  $M_{14}^2$  transition was considered. This assignment was rejected since it goes against the trend of falling wavenumber for the  $M_{14}$  vibration with substituent mass. Instead, we assign  $M_{14}^2$  to the weak feature at  $362\text{ cm}^{-1}$ , which has the added advantage that it allows us to identify the band at  $278.5\text{ cm}^{-1}$  with the  $M_{14}M_{20}$  combination transition – a corresponding band was seen in  $\text{ClBz}$ .<sup>2</sup> Further, as will be seen below, it is then straightforward to identify corresponding vibrations in  $\text{BrBz-}h_5$  which also have expected trends when comparing with  $\text{FBz}$  and  $\text{ClBz}$ . We note that Prakash and Singh<sup>14</sup> attributed a band at  $360\text{ cm}^{-1}$  to an overtone of a vibration with  $a_2$  symmetry, which is consistent with the assignment offered here. This then leaves us requiring an assignment of the  $462\text{ cm}^{-1}$  band. A clue to this comes from the calculated wavenumbers, the wavenumber value of  $M_{14}$ , and the corresponding spectrum of  $\text{ClBz}$ . In the latter, the  $M_{29}$  vibration is in FR with the  $M_{14}M_{19}$  combination, which is almost isoenergetic, and two very close bands of almost the same intensity result. We assign the  $462\text{ cm}^{-1}$  feature here to  $M_{14}M_{19}$ , which we assume is shifted from its non-perturbed value by FR. It is also possible to obtain a wavenumber for  $M_{19}$  from the calculations and comparing with the calculated and experimental values in  $\text{ClBz}$ . This leads us to expect the  $M_{19}$  vibration at  $\sim 310\text{ cm}^{-1}$ , and hence the  $M_{14}M_{19}$  vibration should appear at  $\sim 491\text{ cm}^{-1}$ . With anharmonicity, FR and uncertainty in the values, we feel this assignment of the  $462\text{ cm}^{-1}$  is reasonable, but clearly further evidence from dispersed fluorescence or ZEKE



spectroscopy is needed to confirm this assignment. As will be noted later, the estimated value of  $M_{19}$  suggests the overtone (seen for BrBz- $d_5$ ) may be obscured by the  $M_{10}$  transition.

At  $521.5\text{ cm}^{-1}$  the intense, vibronically-allowed  $M_{29}$  transition appears and as noted above, this vibration is in Fermi resonance with the  $M_{14}M_{19}$  combination in ClBz- $h_5$ , but the mass effect has shifted the latter to lower wavenumber, but it still appears in the spectrum here. This is followed by a weak feature at  $539.0\text{ cm}^{-1}$  that can be assigned to  $M_{11}M_{30}$  and then the commonly-observed  $M_{10}$  at  $623.0\text{ cm}^{-1}$ . The weak feature at  $733.0\text{ cm}^{-1}$  is in the correct position to be the  $M_{20}^2M_{29}$  transition, while the  $741.0\text{ cm}^{-1}$  band is tentatively assigned to the  $M_{13}M_{14}$  combination.

Walerstein<sup>12</sup> notes the appearance of a band with a value of  $242\text{ cm}^{-1}$  (assigned to  $M_{30}$  here), which was thought to correspond to a totally-symmetric vibration. We also note that the  $M_{30}$  band was seen by Dietz et al. at  $240.5\text{ cm}^{-1}$ ,<sup>16</sup> but they assigned this to an overtone in that work; interestingly, Prakash and Singh<sup>14</sup> offered a similar assignment. However, the calculated values and comparison with previous work on FBz and ClBz (confirmed by dispersed fluorescence and/or zero-kinetic energy, ZEKE, spectroscopy – see refs. 1 and 2) suggest the present assignment to  $M_{30}$  ( $b_2$  symmetry) is the correct one.

Dietz et al.<sup>16</sup> and Prakash and Singh<sup>14</sup> also saw the  $M_{11}$  feature and assigned it to the  $\nu_{6a}$  Wilson mode; however, as Table 1 shows the  $M_{11}$  mode is of very mixed Wilson-mode character and in fact it is the  $M_{10}$  mode that corresponds to the Wilson  $\nu_{6a}$  mode. The  $M_{10}$  mode itself was reported in ref. 16 as Wilson mode 1 at  $620.8\text{ cm}^{-1}$ , which is in agreement with our spectrum, and such a feature was also seen in ref. 14. In general, reasonable agreement is seen in this range with the results of Klimusheva et al.<sup>15</sup> for the vibrational wavenumbers that they were able to deduce from their 20 K vapour absorption spectrum, but the values for  $M_{11}$ ,  $M_{14}$  and  $M_{30}$  are somewhat higher than other reported values and those obtained here (see Table 3).

The assignment of the  $M_{29}$  band at  $\sim 520\text{ cm}^{-1}$  is consistent with the assignment in ref. 16 to the close-to-pure  $\nu_{6b}$  Wilson mode and to a non-totally-symmetric vibration by Walerstein;<sup>12</sup> a vibration of  $\sim 520\text{ cm}^{-1}$  was also reported in ref. 13. The assignment of  $M_{29}$  has also been confirmed in the REMPI-photoelectron spectroscopy (REMPI-PES) study of Walter et al.,<sup>9</sup> which we shall comment on further below, and in the absorption study of Prakash and Singh.<sup>14</sup>

In a short report, Sreeramamurthy<sup>13</sup> observed a difference wavenumber of  $221\text{ cm}^{-1}$ , but did not assign this. The same spacing (albeit  $225\text{ cm}^{-1}$ ) was reported by Prakash and Singh<sup>14</sup> who attributed it to a 1–1 hot band, suggesting  $M_{14}^1$ , which is consistent with the ground and excited state values given here in Tables 2 and 3.

*b. BrBz- $d_5$*

As far as we are aware, there have been no previous studies of the BrBz- $d_5$  isotopologue, and so the assignment of this spectrum relies on the calculated vibrational wavenumbers/isotopic shifts and our previous assignments of the two lighter monohalobenzenes.<sup>1,2</sup> In the region below 300  $\text{cm}^{-1}$  the three vibrations observed in BrBz- $h_5$  are present with relatively similar positions, consistent with the small calculated isotopic shifts for these. A band at 309.1  $\text{cm}^{-1}$  is assigned as  $(M_{14}^2)^d$ , based on the expected large H/D isotopic shift and consistent with the behaviour seen previously for FBz and ClBz. This would give a predicted position for the  $(M_{14}M_{20})^d$  combination as  $\sim 254 \text{ cm}^{-1}$ , so the weak band at 249.1  $\text{cm}^{-1}$  can be cautiously assigned to this band, with the difference attributable to anharmonicity. We note that the  $M_{11}$  band is slightly red shifted in the  $^{81}\text{BrBz-}d_5$  spectrum (not shown), consistent with the present calculated values (see supplementary material<sup>28</sup>).

The  $M_{29}^d$  feature appears strongly at 493.6  $\text{cm}^{-1}$ , and we note that there is no obvious band that can be assigned to  $(M_{14}M_{19})^d$  which is straightforwardly attributed to its being too separated in wavenumber, with the combination expected at  $\sim 419 \text{ cm}^{-1}$ ; a similar picture emerged for ClBz.<sup>2</sup>

To slightly higher wavenumber there is a small group of features, which we have marked  $\alpha$ . From the calculated wavenumbers, and the spectrum of BrBz- $h_5$ , we would expect the  $(M_{11}M_{30})^d$  transition to appear here, and this would be expected at  $\sim 518 \text{ cm}^{-1}$ . Since the  $M_{11}M_{30}$  transition was weak in BrBz- $h_5$ , we conclude there is a FR in BrBz- $d_5$  between  $(M_{11}M_{30})^d$  and  $M_{29}^d$ . On the basis of the vibrations assigned thus far, the attribution of other vibrations close to 518  $\text{cm}^{-1}$  seems not to be possible. Insight is achieved, however, with the assignment of the 560.1  $\text{cm}^{-1}$  feature to  $(M_{13}M_{14})^d$ , consistent with the tentative assignment of a corresponding band in BrBz- $h_5$  and the calculated shifts upon deuteration; this gives a value for  $M_{13}^d$  of  $\sim 406 \text{ cm}^{-1}$ . As a consequence of this, an assignment of a contributor to feature  $\alpha$  of  $(M_{13}M_{20})^d$  can be explored. Although the expected wavenumber of this transition based on half the value for the  $M_{20}^d$  overtone seems too low, it should be remembered that the latter vibration is likely to be quite anharmonic. In fact the calculated harmonic value of  $M_{20}^d$  is 112  $\text{cm}^{-1}$ , giving an expected position of  $(M_{13}M_{20})^d$  of 518  $\text{cm}^{-1}$ , and so this is a plausible contributor to feature  $\alpha$ . Additionally, we note that this combination is of  $b_2$  symmetry and so could be in Fermi resonance with  $M_{29}^d$  and/or  $(M_{11}M_{30})^d$ , perhaps explaining why it is seen in the spectrum of BrBz- $d_5$  and not in that of BrBz- $h_5$ . To slightly higher wavenumber is a band at 528.1  $\text{cm}^{-1}$  whose assignment can be deduced from the equivalent spectrum for ClBz- $d_5$  where the  $(M_{19}^2)^d$  transition was identified, giving a value for  $M_{19}^d$  that was also about 30  $\text{cm}^{-1}$  lower than the calculated value. The calculated value of 297  $\text{cm}^{-1}$  for BrBz- $d_5$  would suggest a  $M_{19}^d$  wavenumber of  $\sim 267 \text{ cm}^{-1}$ , and hence a transition to the overtone,  $(M_{19}^2)^d$ , at  $\sim 528 \text{ cm}^{-1}$  can be tentatively assigned. (With this assignment, we can use the differences in the calculated and experimental values for  $M_{19}^d$  to estimate the value for  $M_{19}$ , obtaining a value of 311  $\text{cm}^{-1}$ , suggesting  $M_{19}^2$  could be lying underneath the  $M_{10}$  feature, with there being some indication of a second feature there; this is also consistent with the position of the  $M_{14}M_{19}$  mentioned above.)

The band at 604.1  $\text{cm}^{-1}$  can be assigned to  $M_{10}^d$  and it is interesting to note that this is quite weak; in FBz- $d_5$  and ClBz- $d_5$  the same transition was also weak and this was attributed to its being involved in complex Fermi

resonances, but this seems not to be the case here. The only other band of note in this region is one at 714.1  $\text{cm}^{-1}$ , with  $(M_{29}M_{30})^d$  being our favoured assignment.

## 2. Medium wavenumber range (750-1050 $\text{cm}^{-1}$ )

### a. BrBz- $h_5$

This region is dominated by three main features at  $\sim 934 \text{ cm}^{-1}$ ,  $\sim 963 \text{ cm}^{-1}$  and  $\sim 1023 \text{ cm}^{-1}$  and interestingly there is very little structure in the range 750–900  $\text{cm}^{-1}$ . With regard to comparison with previous spectra and calculated fundamentals, the main expected contributors to these features are  $M_8$ ,  $M_9$  and  $M_6$ , respectively. The agreement between the calculated wavenumbers for the  $M_8$  and  $M_9$  vibrations and that observed is good, while that for  $M_6$  is calculated to be  $\sim 30 \text{ cm}^{-1}$  too low, as was seen previously for the two lighter monosubstituted benzenes.<sup>1,2</sup> The two higher-wavenumber features have a width consistent with a single contribution, and so these are safely assigned as labelled in Figure 6; the lowest wavenumber feature has a width suggestive of further contributors than  $M_8$ : we have marked this feature  $\beta$ . One obvious contributor to this feature, based on previous work, would be  $M_{10}M_{11}$ , which also has  $a_1$  symmetry and so could be in FR with the  $M_8$  vibration. It is expected at  $\sim 920 \text{ cm}^{-1}$ , calculated from the sum of the wavenumbers of the two contributors, with both anharmonicity and FR expected to push the band lower in wavenumber. We conclude that this transition is associated with a weak feature on the low wavenumber ( $\sim 918 \text{ cm}^{-1}$ ) side of region  $\beta$ , which is consistent with a small red shift seen for this feature in the  $^{81}\text{BrBz-}h_5$  spectrum (not shown). There is no obvious other fundamental of  $a_1$  or  $b_2$  symmetry that could contribute to region  $\beta$ , nor is there an overtone, but comparison with the corresponding FBz spectrum suggests the  $M_{15}M_{20}$  combination band could be contributing to the central region at  $\sim 931 \text{ cm}^{-1}$ , and that the corresponding vibration is in FR with the  $M_8$  vibration. This would give a value for the  $M_{15}$  fundamental of  $\sim 825 \text{ cm}^{-1}$ , which is in reasonable agreement with the calculated value of  $843 \text{ cm}^{-1}$ , considering that the calculated value in FBz was also not in such good agreement with experiment. The value is not in such good agreement with the value reported by Klimusheva et al.,<sup>15</sup> but the lack of detail and spectra, together with the discrepancies noted above, lead us to doubt their value. It is interesting to note that the  $M_{15}M_{20}$  combination was also in FR with the  $M_8$  vibration in FBz, while in ClBz this was not the case. Similarly,  $M_{15}M_{20}$  was in FR with the  $M_9$  in toluene- $d_3$ ,<sup>29</sup> indicating that this vibration can interact with the  $M_8$  and  $M_9$  modes if it happens to be in energetic proximity.

The three main bands corresponding to  $M_8$ ,  $M_9$  and  $M_6$  were seen in the study by Dietz et al.<sup>16</sup> although the more complicated nature of the feature at  $\sim 935 \text{ cm}^{-1}$  was not noted. These three bands were also employed to record REMPI-PES spectra by Walter et al.,<sup>9</sup> although the stated wavenumber for the  $M_8$  feature seems to be incorrect, but the spectra suggest this was indeed the intermediate state employed (see later discussion of the photoelectron spectra). We note that the assignment of the  $961 \text{ cm}^{-1}$  band was given as the Wilson overtone  $\nu_{18a}^2$ , which differs from the present assignment and that of ref. 16, but this seems to have been a typographical error (see

below), and this should be a transition to a fundamental vibration. We also note that different Wilson (Varsányi) labels were also used for the  $M_8$ ,  $M_9$  and  $M_6$  modes between refs. 9 and 16 (see Table 1).

Both Walerstein<sup>12</sup> and Sreeramamurty<sup>13</sup> note vibrations with wavenumbers of 933, 963 and 1020  $\text{cm}^{-1}$ , which correspond to  $M_8$ ,  $M_9$  and  $M_6$ , respectively, and very similar values are reported by Klimusheva et al.<sup>15</sup> Additionally, the latter study also reports a value for  $M_{12}$ , but this is in very poor agreement with our calculated value. We did not see any contributions from this vibration in the present work, and neither have any previous studies.

### *b. BrBz- $d_5$*

We now move onto the spectrum of BrBz- $d_5$ , which has more features in it. First, from our previous work<sup>1,2</sup> we expect there to be a significant red shift of the  $M_8$  vibration upon deuteration, with smaller red shifts for the  $M_6$  and  $M_9$  vibrations. It is thus relatively straightforward to assign the band at 921.1  $\text{cm}^{-1}$  to  $M_9^d$  and that at 996.6  $\text{cm}^{-1}$  to  $M_6^d$ . Interestingly, the identification of the  $M_6^d$  and  $M_8^d$  vibrations from our calculations is not as transparent for BrBz- $d_5$  (see comments above), but fortunately, their wavenumbers and isotopic shifts are different enough for the assignment to be straightforward, particularly by comparison with our previous FBz and ClBz spectra. (Recall that the  $M_6$  and  $M_8$  motions are quite similar, with the main difference being the larger motion of the substituent in  $M_6$ , as the mass of the substituent approaches that of the ring.<sup>10</sup>) The calculated wavenumbers and comparison with the appearance of the two isotopologue spectra for each of FBz and ClBz then allowed the transition at 779.1  $\text{cm}^{-1}$  to be assigned to  $M_8^d$ .

Moving onto the other features, a band at 796.1  $\text{cm}^{-1}$  can be associated with  $(M_{14}^2M_{29})^d$ , consistent with the appearance of such a band in the BrBz- $h_5$  spectrum. There are then two features to the red of the  $M_9^d$  band at 895.1  $\text{cm}^{-1}$  and 906.6  $\text{cm}^{-1}$ , the first is an excellent match for the expected position of the  $(M_{10}M_{11})^d$  transition, and this feature also red shifts by  $\sim 1.5 \text{ cm}^{-1}$  for  $^{81}\text{BrBz-}d_5$ . The second band is then  $(M_{10}M_{14}^2)^d$  and the corresponding vibration may be in FR with  $M_9^d$ . The band to the red of  $M_6^d$  at 977.1  $\text{cm}^{-1}$  is in the correct position to be  $(M_8M_{20}^2)^d$  and the two vibrations could also form a FR.

### **3. High wavenumber range (1050-3000 $\text{cm}^{-1}$ )**

As we move higher in wavenumber, more and more candidates arise for features, and there is the possibility of complications arising from anharmonic shifts and FR; for these reasons we refrain from a detailed discussion of the assignment of this higher region, but note the following points. It is relatively straightforward to pick out overtones and combinations involving the intense features, particularly with the  $M_8$  and  $M_9$  pair of features for BrBz- $h_5$ . Indeed, once these are provisionally identified much of the main structure of the high-wavenumber regions is assigned. The assignments are summarized in Tables 4 and 5, and selected ones are also labelled in

Figure 1. Some high-wavenumber ( $< 1580 \text{ cm}^{-1}$ ) features were also identified in the work of Dietz et al.<sup>16</sup> using Wilson labels, and their assignments largely (but not completely) match those here, with the nomenclature change. A number of features occur close together, such as those involving the  $M_8^2$ ,  $M_8M_9$  and  $M_9^2$  together with the  $M_6M_8$  and  $M_6M_9$ ; clearly combination bands of these with another vibration will also appear close together, and we have indicated two such in Figure 1. With regard to previous work, we note that Prakash and Singh<sup>14</sup> assigned a good number of the bands up to  $4382 \text{ cm}^{-1}$  and, although there are shifts of a few  $\text{cm}^{-1}$  from the present values, many assignments are consistent with those here. One interesting point is that a feature at  $3082 \text{ cm}^{-1}$  was observed, which has  $b_2$  symmetry and it was hypothesised that this could be due to a totally-symmetric fundamental vibration of  $2564 \text{ cm}^{-1}$  that was in combination with  $M_{29}$ ; such a spacing was also identified by Walterstein.<sup>12</sup> No such vibration is obvious from our calculations, but instead we suggest the  $3082 \text{ cm}^{-1}$  feature could be assigned to the  $b_2$  mode,  $M_{22}$ .

Finally, Klimusheva et al.<sup>15</sup> reported values for  $M_7$ ,  $M_{23}$ ,  $M_{24}$ ,  $M_{25}$  and  $M_{27}$  that are in moderately good agreement with our calculated values, but we did not see any contributions from these vibrations in the present work, nor have they been reported by others.

By analogy, even though the  $M_8$  and  $M_9$  pair does not appear for BrBz- $d_5$ , we can pick out the corresponding combinations involving  $M_9^d$  and have labelled these in the inverted trace of Figure 1. Clearly many other contributions are appearing in these regions of the spectrum.

#### 4. Cation

The Duschinsky matrix for the  $-h_5$  isotopologue showing the relationship between  $S_0$  and  $D_0^+$  vibrations for BrBz is shown in Figure 7a, and that for the  $S_1$  and  $D_0^+$  vibrations in Figure 7b. The appearance of these suggests that the vibrational motion in the cation is largely the same as in each of the two neutral states, although some of these will show deviation. Based on this and previous work, for most cases we would expect a  $\Delta v = 0$  propensity rule to work well for the  $D_0^+ \leftarrow S_1$  ionization, so that the selected intermediate vibrational level in a REMPI-PES experiment would correspond to that of the most intense cation band.

We have calculated the vibrational wavenumbers of BrBz- $h_5^+$  and present these in Table 6; for completeness, we also present the BrBz- $d_5^+$  values. Referring to Walter et al.'s paper,<sup>9</sup> we have noted above that some of the assignments they offered are neither consistent with those here, nor with those in ref. 16; however, the observed structure in the REMPI-PES spectra should help elucidate this. First we note that exciting via the origin yielded a progression of bands with a spacing of  $320 \text{ cm}^{-1}$ , which matches our calculated  $323 \text{ cm}^{-1}$  value for  $M_{11}^+$  extremely well. Walter et al. assigned this as Wilson mode  $\nu_{6a}$ , but we have noted above (see Table 1) and elsewhere<sup>10</sup> that  $M_{11}$  is quite mixed in the monosubstituted benzenes, and that  $\nu_{6a}$  is essentially  $M_{10}$  for the heavier species. When exciting via the  $M_{29}$  level a series of bands with a spacing of  $540 \text{ cm}^{-1}$  was observed,<sup>9</sup> which matches very well our calculated value of  $534 \text{ cm}^{-1}$  for  $M_{29}^+$ . They also observed a spacing of  $950 \text{ cm}^{-1}$ , which is in best agreement with our value for  $M_8^+$ . Progressions of  $950 \text{ cm}^{-1}$  and  $320 \text{ cm}^{-1}$  were seen when

exciting via the  $M_8$  intermediate level (recall we noted there seems to have been an error in the reporting of the wavenumber of that transition), which match the spacings given above; additionally, another spacing of  $1530\text{ cm}^{-1}$  was observed, which best matches our calculated  $M_4^+$  value. Excitation of the  $M_9$  mode (erroneously given as an overtone in Table 1 of ref. 9, but as a fundamental,  $\nu_{18a}$ , in the text and in the caption of Figure 7) gives progressions involving spacings of  $320$  and  $980\text{ cm}^{-1}$ , with the latter being assignable as  $M_9^+$  from our calculated values in Table 6.

There is much confusion with the excitation of the intermediate level at what Walter et al.<sup>9</sup> cite as  $1060\text{ cm}^{-1}$  above the  $S_1$  origin, which Dietz et al.<sup>16</sup> locate at  $1019\text{ cm}^{-1}$ , in excellent agreement with our position (Table 4). Further, owing to a lack of structure below the  $\Delta\nu = 0$  region in their REMPI-PES spectrum, Walter et al.<sup>9</sup> tentatively reassign this level as Wilson mode  $\nu_{9b}$  (but maintain a  $\nu_{9a}$  label in other places in the paper). However, the spacings ( $134\text{ meV}$ ) they see of  $1080\text{ cm}^{-1}$  (but mistyped as  $1180\text{ cm}^{-1}$  therein) are in best agreement with those for  $M_6^+$  and so confirm an assignment of the intermediate level to  $M_6$  and not to a  $b_2$  symmetry vibration

Kwon et al.<sup>20</sup> recorded one-photon, mass-analyzed threshold ionization (MATI) spectra of BrBz, noting largest shifts of only a few  $\text{cm}^{-1}$  between some of the vibrations between the  $^{79}\text{Br}$  and  $^{81}\text{Br}$  isotopologues. Rich structure was seen in the spectrum and assigned to various vibrational modes using Wilson notation, with the derived wavenumbers included in Table 6. In including these, we have associated them with an  $M_i^+$  label on the basis of previous discussion and on the basis of the symmetry. As can be seen, for many of the modes good agreement is seen with the calculated values, but there are some anomalies. The  $M_{29}^+$  value of  $593\text{ cm}^{-1}$  seems far from the REMPI-PES value and our calculated value, and the  $M_{23}^+$  value of  $1523\text{ cm}^{-1}$  is also far from our calculated value. The proposed value of  $3083\text{ cm}^{-1}$  agrees best with our  $M_3^+$  value. The assignment of the  $1008\text{ cm}^{-1}$  feature to  $M_9^+$  is unclear because it does not match the REMPI-PES value well. Since the resolution is much better in the MATI study, and the latter value is also closer to the value from the conventional PES studies by Potts et al. and Holland et al.,<sup>18,19</sup> then we take this value as the more reliable. We also note that the conventional PES studies give values for  $M_{11}^+$  that match other experimental and the present calculated values well.

#### D. Iodobenzene

There is a trend for the lifetimes of the  $S_1$  state to shorten with increasing mass of the halogen, attributable to intersystem crossing (ISC) and predissociation in the cases of FBz, ClBz and BrBz. Additionally, no LIF or REMPI spectrum appears to have been achievable for IBz, attributed to this short lifetime,<sup>16</sup> caused by internal conversion (IC) to a repulsive region of a singlet  $n\sigma^*$  state (in contrast to ISC for the other monohalobenzenes);<sup>30,31</sup> however, it was possible for Kwon et al.<sup>20</sup> to record a one-colour MATI spectrum of iodobenzene, since the predissociating  $S_1$  state is bypassed. We did not attempt to record a REMPI spectrum of IBz in the present work; however, we here briefly consider the vibrational assignment of the  $S_0$  and  $D_0^+$  states.

The  $S_0$  state vibrational wavenumbers have been reported by Whiffen<sup>6</sup> and Griffiths and Thompson,<sup>7</sup> and were assigned Wilson-like labels by Varsányi<sup>5</sup> (with some changes in assignments); we briefly discussed the assignments in terms of the  $M_i$  nomenclature in ref. 10, noting there that Wilson labels are inappropriate for many of the vibrations, and the inconsistency in assigning labels through the monohalobenzene series by Varsányi. In Table 7 we summarize the experimental vibrational wavenumbers, together with the present B3LYP/aug-cc-pVTZ values. As can be seen, the agreement between experiment and the present calculated values is extremely good in all cases; there is also agreement with the assignment presented in ref. 10. The only point worth emphasising is the switch in the wavenumber ordering of modes  $M_6$  and  $M_7$ , which also occurs for ClBz and BrBz (see above), noted in ref. 10, but the motion of the corresponding vibrations for the series FBz  $\rightarrow$  IBz being very similar in all cases.

Moving onto the vibrations for  $S_0$  IBz- $d_5$ , again we see that there is very good agreement with the experimental values presented by Nanney et al.<sup>21</sup> (which were given Wilson-like labels by Varsányi,<sup>5</sup> but these are inappropriate and do not match those given to FBz- $d_5$ ). The assignment in terms of  $M_i$  labels is relatively clear, as may be seen by the close-to-diagonal form of the Duschinsky matrix in Figure 8a and also the fact that the  $M_i$  labels have been shown to be appropriate for the  $S_0$  state of IBz- $h_5$  in ref. 10. As with BrBz (and ClBz), there is some change in the motion of some vibrations as a result of the deuteration; however, the majority of the motions are close to those of IBz- $h_5$ . The agreement between the calculated and experimental wavenumber values is again very good in all cases.

We present the calculated values for the cation in Table 8 for both IBz- $h_5^+$  and IBz- $d_5^+$ . There seems to be no experimental data or previous calculations available for IBz- $d_5^+$ , so these are presented for the first time and for completeness. There have been a couple of studies on IBz- $h_5^+$  employing both conventional PES and MATI spectroscopy. The PES studies of Holland et al.<sup>22</sup> and Potts et al.<sup>19</sup> each measured two vibrational separations (see Table 8) that are both expected to be of  $a_1$  symmetry and are straightforwardly associated with the  $M_{11}^+$  and  $M_9^+$  vibrations, respectively.

In the MATI study of Kwon et al.,<sup>20</sup> a number of different vibrations were observed, including the two vibrations seen in the conventional PES studies<sup>19,22</sup> just discussed. We note that an error appears to have been made in the conversion of the value for  $M_{11}^+$ , where a value of  $331\text{ cm}^{-1}$  is cited as coming from ref. 22 whereas in fact this should be  $280\text{ cm}^{-1}$ , and thus in excellent agreement with the  $284\text{ cm}^{-1}$  value obtained from the MATI study, and also in very good agreement with the present calculated value; the Potts et al.<sup>19</sup> value is not cited in that work. The values for  $M_8^+$  agree in the two studies. In Table 8 we have tabulated the vibrational wavenumbers obtained by Kwon et al.<sup>20</sup> As can be seen, very good agreement is obtained in most cases, with the values for  $M_{17}^+$  and  $M_{24}^+$  being in slightly poorer agreement.

## V. CONCLUDING REMARKS

In this paper we have reported the REMPI spectrum of both BrBz-*h*<sub>5</sub> and BrBz-*d*<sub>5</sub> and assigned these in detail up until  $\sim 1050\text{ cm}^{-1}$ , and then the major features thereafter. The present assignment gives a consistent picture of the spectra of FBz, ClBz and BrBz and their -*d*<sub>5</sub> isotopologues and suggests a number of future studies to unpick various Fermi resonances. It is interesting that it is rather straightforward to obtain a good-quality REMPI spectrum of BrBz given the short lifetime that precludes the possibility of obtaining an LIF spectrum; on the other hand, obtaining such a spectrum of IBz appears not to be possible as discussed above, owing to rapid internal conversion.

Our assignments are the first such for BrBz-*d*<sub>5</sub>, while for BrBz-*h*<sub>5</sub> we have discussed the previous suggested assignments, noting some disagreements between them, and presenting our new assignments based on our previous work and quantum chemical calculations. We have also discussed the vibrations of the cations, reassigning where required.

Finally, for IBz we have presented calculated vibrations for the  $S_0$  and  $D_0^+$  states and briefly discussed previous work on these.

In summary, via the present and our previous work on the fluorobenzenes and chlorobenzenes, we have been able to assign corresponding vibrations across the whole monohalobenzene series of molecules, in the  $S_0$ ,  $S_1$  and  $D_0^+$  states, gaining insight into vibrational activity and vibrational couplings.

#### **ACKNOWLEDGEMENTS.**

We are grateful to the EPSRC for funding (grants EP/I012303/1 and L021366/1) and for a studentship to J.P.H. The EPSRC and the University of Nottingham are thanked for studentships to A.A. and W.D.T. We are grateful to the NSCCS for the provision of computer time under the auspices of the EPSRC, and to the High Performance Computer resource at the University of Nottingham.



**Table 1.** Labels for BrBz-*h*<sub>5</sub> S<sub>0</sub> state vibrations.

| Mode Label             | In terms of FBZ <sup>a</sup>  | Wilson/Varsányi |                     |                                  |
|------------------------|---|-----------------|---------------------|----------------------------------|
|                        |   | Ref. 5          | Ref. 9 <sup>b</sup> | In Terms of benzene <sup>c</sup> |
| <i>a</i> <sub>1</sub>  |   |                 |                     |                                  |
| <i>M</i> <sub>1</sub>  | <b><i>M</i><sub>1</sub></b>   | 20a             | 2                   | <b>2</b> ,(7a,13)                |
| <i>M</i> <sub>2</sub>  | <b><i>M</i><sub>2</sub></b>   | 2               | 20a                 | <b>20a</b> ,(2,13)               |
| <i>M</i> <sub>3</sub>  | <b><i>M</i><sub>3</sub></b>   | 13              | 13                  | <b>13</b> ,7a                    |
| <i>M</i> <sub>4</sub>  | <b><i>M</i><sub>4</sub></b>   | 8a              | 8a                  | <b>9a</b>                        |
| <i>M</i> <sub>5</sub>  | <b><i>M</i><sub>5</sub></b>   | 19a             | 19a                 | <b>18a</b>                       |
| <i>M</i> <sub>6</sub>  | <b><i>M</i><sub>6</sub></b> , <i>M</i> <sub>8</sub> ( <i>M</i> <sub>10</sub> )    | 1               | 7a                  | <b>19a</b> , (1)                 |
| <i>M</i> <sub>7</sub>  | <b><i>M</i><sub>7</sub></b> , <i>M</i> <sub>6</sub>                               | 9a              | 9a                  | <b>8a</b>                        |
| <i>M</i> <sub>8</sub>  | <b><i>M</i><sub>8</sub></b> , ( <i>M</i> <sub>10</sub> , <i>M</i> <sub>6</sub> )  | 18a             | 18a                 | <b>1</b> ,19a,12                 |
| <i>M</i> <sub>9</sub>  | <b><i>M</i><sub>9</sub></b>   | 12              | 1                   | <b>12</b> ,1                     |
| <i>M</i> <sub>10</sub> | <b><i>M</i><sub>10</sub></b> , <i>M</i> <sub>11</sub> ( <i>M</i> <sub>6</sub> )   | 6a              | 12                  | <b>6a</b>                        |
| <i>M</i> <sub>11</sub> | <b><i>M</i><sub>11</sub></b> , ( <i>M</i> <sub>10</sub> , <i>M</i> <sub>6</sub> ) | 7a              | 6a                  | (7a, 20a,6a,13,2)                |
| <i>a</i> <sub>2</sub>  |   |                 |                     |                                  |
| <i>M</i> <sub>12</sub> | <b><i>M</i><sub>12</sub></b>  | 17a             | 17a                 | <b>17a</b>                       |
| <i>M</i> <sub>13</sub> | <b><i>M</i><sub>13</sub></b>  | 10a             | 10a                 | <b>10a</b>                       |
| <i>M</i> <sub>14</sub> | <b><i>M</i><sub>14</sub></b>  | 16a             | 16a                 | <b>16a</b>                       |
| <i>b</i> <sub>1</sub>  |   |                 |                     |                                  |
| <i>M</i> <sub>15</sub> | <b><i>M</i><sub>15</sub></b>  | 5               | 5                   | <b>5</b> , 17b                   |
| <i>M</i> <sub>16</sub> | <b><i>M</i><sub>16</sub></b>  | 17b             | 17b                 | 10b,17b                          |
| <i>M</i> <sub>17</sub> | <b><i>M</i><sub>17</sub></b>  | 11              | 10b                 | <b>11</b> , (10b,4)              |
| <i>M</i> <sub>18</sub> | <b><i>M</i><sub>18</sub></b>  | 4               | 4                   | <b>4</b> (11)                    |
| <i>M</i> <sub>19</sub> | <b><i>M</i><sub>19</sub></b>  | 16b             | 16b                 | <b>16b</b> , (11)                |
| <i>M</i> <sub>20</sub> | <b><i>M</i><sub>20</sub></b>  | 10b             | 11                  | (16b, 10b, 17b)                  |
| <i>b</i> <sub>2</sub>  |   |                 |                     |                                  |
| <i>M</i> <sub>21</sub> | <b><i>M</i><sub>21</sub></b>  | 20b             | 20b                 | <b>20b</b>                       |
| <i>M</i> <sub>22</sub> | <b><i>M</i><sub>22</sub></b>  | 7b              | 7b                  | <b>7b</b> ,(20b)                 |
| <i>M</i> <sub>23</sub> | <b><i>M</i><sub>23</sub></b>  | 8b              | 8b                  | <b>9b</b>                        |
| <i>M</i> <sub>24</sub> | <b><i>M</i><sub>24</sub></b>  | 19b             | 19b                 | <b>18b</b> , 3                   |
| <i>M</i> <sub>25</sub> | <b><i>M</i><sub>25</sub></b> , ( <i>M</i> <sub>26</sub> )                         | 14              | 3                   | <b>3</b> , (15)                  |
| <i>M</i> <sub>26</sub> | <b><i>M</i><sub>26</sub></b> , ( <i>M</i> <sub>25</sub> )                         | 3               | 14                  | <b>15</b> , (8b,3)               |
| <i>M</i> <sub>27</sub> | <b><i>M</i><sub>27</sub></b>  | 9b              | 9b                  | <b>14</b> , 8b                   |
| <i>M</i> <sub>28</sub> | <b><i>M</i><sub>28</sub></b>  | 18b             | 15                  | <b>19b</b> , 8b, 14              |
| <i>M</i> <sub>29</sub> | <b><i>M</i><sub>29</sub></b>  | 6b              | 6b                  | <b>6b</b>                        |
| <i>M</i> <sub>30</sub> | <b><i>M</i><sub>30</sub></b>  | 15              | 18b                 | (8b, 19b)                        |

<sup>a</sup> *M*<sub>*i*</sub> modes of BrBz-*h*<sub>5</sub> expressed in terms of those of FBZ-*h*<sub>5</sub>. Values outside parentheses have mixing coefficients > 0.2 and are termed major contributions, with bolded values being dominant contributions (mixing coefficients > 0.5). Those inside parentheses are minor contributions, and have values between 0.05 and 0.2. If there is more than one contribution of each type, these are given in numerical order. Vibrations with a mixing coefficient < 0.05 are ignored.

<sup>b</sup> Vibrational assignment is taken from Ref. 9 – although attributed to the original Varsányi work therein, the assignments are actually different for a number of the vibrations.

<sup>c</sup> *M*<sub>*i*</sub> modes of BrBz-*h*<sub>5</sub> expressed in terms of those of benzene. Values outside parentheses have mixing coefficients > 0.2 and are termed major contributions, with bolded values being dominant contributions (mixing coefficients > 0.5). Those inside parentheses are minor contributions, and have values between 0.05 and 0.2. If there is more than one contribution of each type, these are given in numerical order. Vibrations with a mixing coefficient < 0.05 are ignored.

**Table 2.** Assignments, calculated and experimental vibrational wavenumbers ( $\text{cm}^{-1}$ ) for the  $S_0$  state of  $^{79}\text{BrBz-}h_5$  and  $^{79}\text{BrBz-}d_5$ .

| $^{79}\text{BrBz-}h_5$ |                        |                      |                       | $^{79}\text{BrBz-}d_5$ |                        |                         |
|------------------------|------------------------|----------------------|-----------------------|------------------------|------------------------|-------------------------|
| Mode Label             | Calculated             |                      | Experimental          | Mode Label             | Calculated             | Experimental            |
|                        | This work <sup>a</sup> | Ref. 10 <sup>b</sup> | IR/Raman <sup>c</sup> |                        | This work <sup>a</sup> | IR/Raman <sup>d</sup>   |
| $a_1$                  |                        |                      |                       |                        |                        |                         |
| $M_1$                  | 3109                   | 3212                 | 3069                  | $M_1^d$                | 2304                   | 2296                    |
| $M_2$                  | 3097                   | 3200                 | 3050                  | $M_2^d$                | 2291                   | 2275 <sup>e</sup>       |
| $M_3$                  | 3077                   | 3178                 | 3029                  | $M_3^d$                | 2269                   | 2270                    |
| $M_4$                  | 1567                   | 1616                 | 1580                  | $M_4^d$                | 1530                   | 1551                    |
| $M_5$                  | 1463                   | 1489                 | 1473                  | $M_5^d$                | 1328                   | 1346                    |
| $M_6$                  | 1052                   | 1080                 | 1070                  | $M_6^d$                | 995                    | 1020                    |
| $M_7$                  | 1164                   | 1191                 | 1176                  | $M_7^d$                | 853                    | 865                     |
| $M_8$                  | 1009                   | 1036                 | 1020                  | $M_8^d$                | 815                    | 817 or 826 <sup>f</sup> |
| $M_9$                  | 988                    | 1003                 | 1001                  | $M_9^d$                | 948                    | 958                     |
| $M_{10}$               | 662                    | 676                  | 669                   | $M_{10}^d$             | 633                    | 644                     |
| $M_{11}$               | 305                    | 312                  | 315                   | $M_{11}^d$             | 298                    | 305                     |
| $a_2$                  |                        |                      |                       |                        |                        |                         |
| $M_{12}$               | 961                    | 977                  | 963                   | $M_{12}^d$             | 783                    | 760                     |
| $M_{13}$               | 825                    | 836                  | 832                   | $M_{13}^d$             | 642                    | 680                     |
| $M_{14}$               | 401                    | 415                  | 409                   | $M_{14}^d$             | 348                    | 350                     |
| $b_1$                  |                        |                      |                       |                        |                        |                         |
| $M_{15}$               | 980                    | 1000                 | 988                   | $M_{15}^d$             | 816                    | 817                     |
| $M_{16}$               | 902                    | 914                  | 903                   | $M_{16}^d$             | 742                    | 743                     |
| $M_{17}$               | 732                    | 746                  | 735                   | $M_{17}^d$             | 607                    | 614                     |
| $M_{18}$               | 677                    | 701                  | 681                   | $M_{18}^d$             | 538                    | 543                     |
| $M_{19}$               | 456                    | 472                  | 458                   | $M_{19}^d$             | 401                    | 403                     |
| $M_{20}$               | 162                    | 168                  | 181                   | $M_{20}^d$             | 152                    | 172                     |
| $b_2$                  |                        |                      |                       |                        |                        |                         |
| $M_{21}$               | 3106                   | 3210                 | 3069                  | $M_{21}^d$             | 2299                   | 2280                    |
| $M_{22}$               | 3085                   | 3186                 | 3056                  | $M_{22}^d$             | 2278                   | 2270                    |
| $M_{23}$               | 1573                   | 1623                 | 1577                  | $M_{23}^d$             | 1538                   | 1541                    |
| $M_{24}$               | 1432                   | 1458                 | 1445                  | $M_{24}^d$             | 1304                   | 1316                    |
| $M_{25}$               | 1306                   | 1341                 | 1323                  | $M_{25}^d$             | 1017                   | 1012                    |
| $M_{26}$               | 1275                   | 1316                 | 1264                  | $M_{26}^d$             | 1271                   | 1278                    |
| $M_{27}$               | 1146                   | 1172                 | 1159                  | $M_{27}^d$             | 831                    | 841                     |
| $M_{28}$               | 1064                   | 1092                 | 1068                  | $M_{28}^d$             | 809                    | 800 <sup>e</sup>        |
| $M_{29}$               | 608                    | 621                  | 615                   | $M_{29}^d$             | 583                    | 586                     |
| $M_{30}$               | 240                    | 249                  | 254                   | $M_{30}^d$             | 226                    | 238                     |

<sup>a</sup> B3LYP/aug-cc-pVTZ values, scaled by 0.97

<sup>b</sup> B3LYP/aug-cc-pVDZ, unscaled.

<sup>c</sup> From ref. 6 (see text).

<sup>d</sup> Ref. 21.

<sup>e</sup> Estimated value from ref. 21.

<sup>f</sup> In ref. 21, a band at  $817\text{ cm}^{-1}$  was observed in the IR spectrum, but one at  $826\text{ cm}^{-1}$  was observed in the Raman one.

**Table 3.** Assignments, calculated and experimental vibrational wavenumbers ( $\text{cm}^{-1}$ ) for the  $S_1$  states of  $^{79}\text{BrBz-}h_5$  and  $^{79}\text{BrBz-}d_5$ .

| $^{79}\text{BrBz-}h_5$ |                        |                    |                      |                     |                      |                   | $^{79}\text{BrBz-}d_5$ |                        |                    |
|------------------------|------------------------|--------------------|----------------------|---------------------|----------------------|-------------------|------------------------|------------------------|--------------------|
| Mode Label             | Calculated             | Experimental       |                      |                     |                      | Ref. 14           | Mode Label             | Calculated             | Experimental       |
|                        | This work <sup>a</sup> | This work          | Ref. 16 <sup>b</sup> | Ref. 9 <sup>c</sup> | Ref. 15 <sup>d</sup> |                   |                        | This work <sup>a</sup> | This work          |
| $a_1$                  |                        |                    |                      |                     |                      |                   |                        |                        |                    |
| $M_1$                  | 3135                   |                    |                      |                     |                      |                   | $M_1^d$                | 2320                   |                    |
| $M_2$                  | 3115                   |                    |                      |                     |                      |                   | $M_2^d$                | 2301                   |                    |
| $M_3$                  | 3079                   |                    |                      |                     |                      |                   | $M_3^d$                | 2271                   |                    |
| $M_4$                  | 1445                   |                    |                      |                     | 1447                 |                   | $M_4^d$                | 1394                   |                    |
| $M_5$                  | 1401                   |                    |                      |                     |                      |                   | $M_5^d$                | 1239                   |                    |
| $M_6$                  | 993                    | 1022.5             | 1019.1               | 1020                | 1017                 | 1019              | $M_6^d$                | 965                    | 996.6              |
| $M_7$                  | 1125                   |                    |                      |                     | 1141                 |                   | $M_7^d$                | 833                    |                    |
| $M_8$                  | 949                    | 934.5              | 931.4                |                     | 929                  | 931               | $M_8^d$                | 787                    | 779.1              |
| $M_9$                  | 974                    | 963.0              | 960.3                | 961                 | 959                  | 961               | $M_9^d$                | 917                    | 921.1              |
| $M_{10}$               | 641                    | 623.0              | 620.8                |                     | 650                  | 620               | $M_{10}^d$             | 614                    | 604.1              |
| $M_{11}$               | 295                    | 297.0              | 294.1                |                     | (333)                |                   | $M_{11}^d$             | 289                    | 290.6              |
| $a_2$                  |                        |                    |                      |                     |                      |                   |                        |                        |                    |
| $M_{12}$               | 612                    |                    |                      |                     | 709                  |                   | $M_{12}^d$             | 511                    |                    |
| $M_{13}$               | 511                    | 560 <sup>e</sup>   |                      |                     |                      |                   | $M_{13}^d$             | 412                    | 405.5 <sup>e</sup> |
| $M_{14}$               | -- <sup>f</sup>        | 181.0 <sup>g</sup> |                      |                     | 231                  | 296               | $M_{14}^d$             | -- <sup>f</sup>        | 154.6 <sup>g</sup> |
| $b_1$                  |                        |                    |                      |                     |                      |                   |                        |                        |                    |
| $M_{15}$               | 843                    | 825.4 <sup>e</sup> |                      |                     | 871                  |                   | $M_{15}^d$             | 711                    |                    |
| $M_{16}$               | 680                    |                    |                      |                     |                      | 678 <sup>h</sup>  | $M_{16}^d$             | 581                    |                    |
| $M_{17}$               | 575                    | 579 <sup>g</sup>   |                      |                     |                      |                   | $M_{17}^d$             | 449                    |                    |
| $M_{18}$               | 486                    | 486.8 <sup>e</sup> |                      |                     |                      |                   | $M_{18}^d$             | 393                    |                    |
| $M_{19}$               | 344                    | 311 <sup>i</sup>   |                      |                     |                      |                   | $M_{19}^d$             | 297                    | 264.1 <sup>g</sup> |
| $M_{20}$               | 119                    | 105.6 <sup>g</sup> |                      |                     |                      | 120               | $M_{20}^d$             | 112                    | 99.1 <sup>g</sup>  |
| $b_2$                  |                        |                    |                      |                     |                      |                   |                        |                        |                    |
| $M_{21}$               | 3130                   |                    |                      |                     |                      |                   | $M_{21}^d$             | 2310                   |                    |
| $M_{22}$               | 3106                   |                    |                      |                     |                      | 3082 <sup>j</sup> | $M_{22}^d$             | 2285                   |                    |
| $M_{23}$               | 1426                   |                    |                      |                     | 1476                 |                   | $M_{23}^d$             | 1316                   |                    |
| $M_{24}$               | 1360                   |                    |                      |                     | 1328                 |                   | $M_{24}^d$             | 1199                   |                    |
| $M_{25}$               | 1253                   |                    |                      |                     | 1257                 |                   | $M_{25}^d$             | 996                    |                    |
| $M_{26}$               | 1372                   |                    |                      |                     |                      |                   | $M_{26}^d$             | 1401                   |                    |
| $M_{27}$               | 1121                   |                    |                      |                     | 1199                 |                   | $M_{27}^d$             | 816                    |                    |
| $M_{28}$               | 973                    |                    |                      |                     |                      |                   | $M_{28}^d$             | 775                    |                    |
| $M_{29}$               | 511                    | 521.5              | 518.9                | 517                 | 519                  | 518               | $M_{29}^d$             | 491                    | 493.6              |
| $M_{30}$               | 242                    | 242.0              |                      |                     | 282                  | 234               | $M_{30}^d$             | 228                    | 227.1              |

<sup>a</sup> TDDFT, B3LYP/aug-cc-pVTZ, scaled by 0.97

<sup>b</sup> Dietz et al. REMPI study.

<sup>c</sup> Walter et al. REMPI-PES study.

<sup>d</sup> All values in the vapour phase at 20 K, except for the parenthesised value which was from a 4 K crystalline sample.

<sup>e</sup> Derived from a combination band and so there may be an anharmonic shift..

<sup>f</sup> The  $M_{14}$  mode in the  $S_1$  state is calculated to give unrealistic values, as for the lighter monohalobenzenes, and so is not reported here – see text.

<sup>g</sup> Derived from an overtone band and so there may be an anharmonic shift...

<sup>h</sup> Assigned in the present work from hot bands seen in refs. 13 and 14 – see text.

<sup>i</sup> Tentatively assigned from assuming the overtone is contributing to the feature at  $623 \text{ cm}^{-1}$  – see text.

<sup>j</sup> Reassigned (tentatively) in the present work – see text.

**Table 4.** A summary of the assigned vibrational features from the present work for the  $S_1 \leftarrow S_0$  transition of  $^{79}\text{BrBz-}h_5$

|                | Experimental band ( $\text{cm}^{-1}$ ) <sup>a</sup> | Assignment <sup>b</sup> | This work B3LYP | From experimental fundamental <sup>c</sup> | Overall symmetry |
|----------------|---|-------------------------|-----------------|--|------------------|
|                | 0.0   | $0^0$                   | -               | -  | $a_1$            |
|                | 211.5   | $M_{20}^2$              | 239             | 211.5 <sup>d</sup>                         | $a_1$            |
|                | 242.0   | $M_{30}$                | 242             | 242.0 <sup>d</sup>                         | $b_2$            |
|                | 278.5   | $M_{14}M_{20}$          | - <sup>e</sup>  | 286.6                                      | $b_2$            |
|                | 297.0   | $M_{11}$                | 295             | 297.0 <sup>d</sup>                         | $a_1$            |
|                | 362.0   | $M_{14}^2$              | - <sup>e</sup>  | 362.0 <sup>d</sup>                         | $a_1$            |
|                | 462.0   | $M_{14}M_{19}$          | - <sup>e</sup>  | 492.0                                      | $b_2$            |
|                | 501.5   | $M_{11}M_{20}^2$        | 533             | 508.4                                      | $a_1$            |
|                | 521.5   | $M_{29}$                | 511             | 521.5 <sup>d</sup>                         | $b_2$            |
|                | 539.0   | $M_{11}M_{30}$          | 537             | 539.0                                      | $b_2$            |
|                | 592.5   | $M_{18}M_{20}$          | 606             | 592.5 <sup>d</sup>                         | $a_1$            |
|                | 623.0   | $M_{10}$                | 641             | 623.0 <sup>d</sup>                         | $a_1$            |
|                | 669.5   | $M_{14}M_{18}$          | - <sup>e</sup>  | 667.0                                      | $b_2$            |
|                | 733.0   | $M_{20}^2M_{29}$        | 750             | 732.7                                      | $b_2$            |
|                | 741.0   | $M_{13}M_{14}$          | 691             | 741.0                                      | $a_1$            |
|                | 880.0   | $M_{14}^2M_{29}$        | - <sup>e</sup>  | 883.5                                      | $b_2$            |
|                | 905.5   | $M_{14}M_{18}M_{30}$    | - <sup>e</sup>  | 909.0                                      | $a_1$            |
|                |   | $M_{10}M_{14}M_{20}$    | - <sup>e</sup>  | 909.6                                      | $b_2$            |
| Region $\beta$ | 918.0   | $M_{10}M_{11}$          | 936             | 920.0                                      | $a_1$            |
|                | 931 <sup>f</sup>                                    | $M_{15}M_{20}$          | 963             | 931.0 <sup>d</sup>                         | $a_1$            |
|                | 934 <sup>f</sup>                                    | $M_8$                   | 949             | 934.0 <sup>d</sup>                         | $a_1$            |
|                | 963.0   | $M_9$                   | 974             | 963.0 <sup>d</sup>                         | $a_1$            |
|                | 985.0   | $M_{10}M_{14}^2$        | - <sup>e</sup>  | 985.0                                      | $a_1$            |
|                | 1022.5  | $M_6$                   | 994             | 1022.5 <sup>d</sup>                        | $a_1$            |
|                | 1107.5  | $M_{10}M_{30}^2$        | 1126            | 1107.0                                     | $a_1$            |
|                | 1143.5  | $M_{10}M_{29}$          | 1153            | 1144.5                                     | $b_2$            |
|                | 1150.0  | $M_8M_{20}^2$           | 1187            | 1146.0                                     | $a_1$            |
|                | 1157.5  | $M_{17}^2$              | 1150            | 1157.5                                     | $a_1$            |
|                | 1174.5  | $M_9M_{20}^2$           | 1212            | 1174.5                                     | $a_1$            |
|                | 1176.5  | $M_8M_{30}$             | 1191            | 1176.6                                     | $b_2$            |
|                | 1203.5  | $M_9M_{30}$             | 1216            | 1205.0                                     | $b_2$            |
|                | 1211.0  | $M_{18}^2M_{30}$        | 1198            | 1214.0                                     | $b_2$            |
|                | 1231.5  | $M_8M_{11}$             | 1243            | 1231.6                                     | $a_1$            |
|                | 1258.5  | $M_9M_{11}$             | 1268            | 1260.0                                     | $a_1$            |
|                | 1455.0  | $M_8M_{29}$             | 1460            | 1456.1                                     | $b_2$            |
|                | 1474  | $M_8M_{11}M_{30}$       | 1486            | 1473.6                                     | $b_2$            |
|                | 1482  | $M_9M_{29}$             | 1485            | 1484.5                                     | $b_2$            |
|                | 1498  | $M_9M_{11}M_{30}$       | 1510            | 1502.0                                     | $b_2$            |
|                | 1542  | $M_6M_{29}$             | 1505            | 1544.0                                     | $b_2$            |
|                | 1868  | $M_8^2$                 | 1897            | 1869.2                                     | $a_1$            |
|                | 1898  | $M_8M_9$                | 1922            | 1897.6                                     | $a_1$            |
|                | 1926  | $M_9^2$                 | 1947            | 1926.0                                     | $a_1$            |
|                | 1956  | $M_6M_8$                | 1942            | 1957.1                                     | $a_1$            |
|                | 1986  | $M_6M_9$                | 1967            | 1985.5                                     | $a_1$            |
|                | 2386  | $M_8^2M_{29}$           | 2409            | 2390.7                                     | $b_2$            |
|                | 2414  | $M_8M_9M_{29}$          | 2434            | 2419.1                                     | $b_2$            |
|                | 2440  | $M_9^2M_{29}$           | 2459            | 2447.5                                     | $b_2$            |
|                | 2474  | $M_6M_8M_{29}$          | 2454            | 2478.6                                     | $b_2$            |
|                | 2500  | $M_6M_9M_{29}$          | 2478            | 2507.0                                     | $b_2$            |

|  |      |            |      |        |       |
|--|------|------------|------|--------|-------|
|  | 2892 | $M_6M_8^2$ | 2891 | 2891.7 | $a_1$ |
|  | 2948 | $M_6M_9^2$ | 2941 | 2948.5 | $a_1$ |
|  | 2974 | $M_6^2M_8$ | 2936 | 2979.6 | $a_1$ |

<sup>a</sup> Features above 1460 cm<sup>-1</sup> are quoted to the nearest 1 cm<sup>-1</sup> only since only scans with 2 cm<sup>-1</sup> stepsize were undertaken for this isotopologue.

<sup>b</sup> Selected assignments given for the region > 1000 cm<sup>-1</sup>. If more than one option is given, the assignment is not known definitely.

<sup>c</sup> All values have been computed from experimental fundamentals.

<sup>d</sup> An experimental fundamental is taken from this feature.

<sup>e</sup>  $M_{14}$  calculated B3LYP frequency was unrealistic; see text for details.

<sup>f</sup> Overlapped bands, and so the position is an estimate.

**Table 5.** A summary of the assigned vibrational features from the present work for the  $S_1 \leftarrow S_0$  transition of  $^{79}\text{BrBz-d}_5$

|          | Experimental band ( $\text{cm}^{-1}$ ) <sup>a</sup> | Assignment <sup>b</sup> | This work B3LYP | From experimental fundamentals <sup>c</sup> | Overall symmetry |
|----------|---|-------------------------|-----------------|---|------------------|
|          | 0.0   | $0^0$                   | -               | -   | -                |
|          | 198.1   | $(M_{20}^2)^d$          | 224             | 198.1 <sup>d</sup>                          | $a_1$            |
|          | 227.1   | $M_{30}^d$              | 228             | 227.1 <sup>d</sup>                          | $b_2$            |
|          | 249.1   | $(M_{14}M_{20})^d$      | - <sup>e</sup>  | 253.7                                       | $b_2$            |
|          | 290.6   | $M_{11}^d$              | 289             | 290.6 <sup>d</sup>                          | $a_1$            |
|          | 309.1   | $(M_{14}^2)^d$          | - <sup>e</sup>  | 309.2 <sup>d</sup>                          | $a_1$            |
|          | 487.6   | $(M_{11}M_{20}^2)^d$    | 513             | 488.7                                       | $a_1$            |
|          | 493.6   | $M_{29}^d$              | 491             | 493.6 <sup>d</sup>                          | $b_2$            |
| $\alpha$ | 515.6   | $(M_{13}M_{20})^d$      | 524             | 504.6                                       | $b_2$            |
|          | 518.1   | $(M_{11}M_{30})^d$      | 517             | 517.7                                       | $b_2$            |
|          | 528.1   | $(M_{19}^2)^d$          | - <sup>e</sup>  | 528.1 <sup>d</sup>                          | $a_1$            |
|          | 560.1   | $(M_{13}M_{14})^d$      | - <sup>e</sup>  | 560.1 <sup>d</sup>                          | $a_1$            |
|          | 604.1   | $M_{10}^d$              | 615             | 604.1 <sup>d</sup>                          | $a_1$            |
|          | 714.1   | $(M_{29}M_{30})^d$      | 719             | 720.7                                       | $a_1$            |
|          | 779.1   | $M_8^d$                 | 787             | 779.1 <sup>d</sup>                          | $a_1$            |
|          | 796.1   | $(M_{14}^2M_{29})^d$    | - <sup>e</sup>  | 802.8                                       | $b_2$            |
|          | 895.1   | $(M_{10}M_{11})^d$      | 898             | 894.7                                       | $a_1$            |
|          | 906.6   | $(M_{10}M_{14}^2)^d$    | - <sup>d</sup>  | 915.7                                       | $a_1$            |
|          | 921.1   | $M_9^d$                 | 917             | 921.1 <sup>d</sup>                          | $a_1$            |
|          | 977.1   | $(M_8M_{20}^2)$         | 1011            | 977.3                                       | $a_1$            |
|          | 996.6   | $M_6^d$                 | 965             | 996.6 <sup>d</sup>                          | $a_1$            |
|          | 1086.6  | $(M_8M_{14}^2)^d$       | - <sup>e</sup>  | 1088.3                                      | $a_1$            |
|          | 1093.6  | $(M_{10}M_{29})^d$      | 1106            | 1097.7                                      | $b_2$            |
|          | 1117.1  | $(M_9M_{20}^2)^d$       | 1141            | 1119.3                                      | $a_1$            |
|          | 1147.6  | $(M_9M_{30})^d$         | 1145            | 1148.2                                      | $b_2$            |
|          | 1209.1  | $(M_9M_{11})^d$         | 1206            | 1211.7                                      | $a_1$            |
|          | 1222.6  | $(M_6M_{30})^d$         | 1193            | 1223.7                                      | $b_2$            |
|          | 1225.1  | $(M_9M_{14}^2)^d$       | - <sup>e</sup>  | 1230.1                                      | $a_1$            |
|          | 1286.1  | $(M_6M_{11})^d$         | 1253            | 1287.2                                      | $a_1$            |
|          | 1415.1  | $(M_9M_{29})^d$         | 1408            | 1414.7                                      | $a_2$            |
|          | 1439.6  | $(M_9M_{11}M_{30})^d$   | 1434            | 1438.8                                      | $b_2$            |
|          | 1464.6  | $(M_8M_{18}M_{19})^d$   | - <sup>e</sup>  | 1468.1                                      | $b_2$            |
|          | 1484.6  | $(M_6M_{29})^d$         | 1456            | 1490.2                                      | $b_2$            |
|          | 1843  | $(M_9^2)^d$             | 1834            | 1842.2                                      | $a_1$            |
|          | 2057  | $(M_8^2M_{29})^d$       | 2065            | 2051.8                                      | $b_2$            |
|          | 2067  | $(M_6M_8M_{11})^d$      | 2041            | 2066.3                                      | $a_1$            |
|          | 2277  | $(M_6M_8M_{29})^d$      | 2243            | 2269.2                                      | $b_2$            |
|          | 2335  | $(M_9^2M_{29})^d$       | 2326            | 2335.8                                      | $b_2$            |
|          | 2385  | $(M_6M_8M_{10})^d$      | 2366            | 2379.8                                      | $a_1$            |
|          | 2457  | $(M_9^2M_{10})^d$       | 2449            | 2446.3                                      | $a_1$            |

<sup>a</sup> Features above  $1500 \text{ cm}^{-1}$  are quoted to the nearest  $\text{cm}^{-1}$  as only  $2 \text{ cm}^{-1}$  step size scans were taken of the high wavenumber region for this isotopologue.

<sup>b</sup> Selected assignments given for the region  $> 1000 \text{ cm}^{-1}$ .

<sup>c</sup> All values come from experimental fundamentals.

<sup>d</sup> An experimental fundamental is taken from this feature.

<sup>e</sup>  $M_{14}^d$  calculated B3LYP frequency is unphysical; see text for details.

**Table 6.** Assignments, calculated and experimental vibrational wavenumbers ( $\text{cm}^{-1}$ ) for the ground state cation,  $\text{D}_0^+$ , of  $^{79}\text{BrBz-}h_5$  and  $^{79}\text{BrBz-}d_5$ .

| $^{79}\text{BrBz-}h_5^+$ |                        |                            |                          |                  | $^{79}\text{BrBz-}d_5^+$ |                        |
|--------------------------|------------------------|----------------------------|--------------------------|------------------|--------------------------|------------------------|
| Mode Label               | Calculated             | Experimental               |                          |                  | Mode Label               | Calculated             |
|                          | This work <sup>a</sup> | Walter et al. <sup>b</sup> | Kwon et al. <sup>c</sup> | PES <sup>d</sup> |                          | This work <sup>a</sup> |
| $a_1$                    |                        |                            |                          |                  |                          |                        |
| $M_1^+$                  | 3121                   |                            |                          |                  | $M_1^{d+}$               | 2316                   |
| $M_2^+$                  | 3111                   |                            |                          |                  | $M_2^{d+}$               | 2299                   |
| $M_3^+$                  | 3098                   |                            | 3083 <sup>e</sup>        |                  | $M_3^{d+}$               | 2289                   |
| $M_4^+$                  | 1573                   | 1530                       | 1577                     |                  | $M_4^{d+}$               | 1532                   |
| $M_5^+$                  | 1425                   |                            |                          |                  | $M_5^{d+}$               | 1251                   |
| $M_6^+$                  | 1040                   | 1080 <sup>f</sup>          | 1073                     |                  | $M_6^{d+}$               | 1016                   |
| $M_7^+$                  | 1181                   |                            | 1193                     |                  | $M_7^{d+}$               | 854                    |
| $M_8^+$                  | 966                    | 950                        |                          |                  | $M_8^{d+}$               | 801                    |
| $M_9^+$                  | 981                    | 980                        | 1008                     | 1020<br>(1016)   | $M_9^{d+}$               | 933                    |
| $M_{10}^+$               | 669                    |                            | 678                      |                  | $M_{10}^{d+}$            | 639                    |
| $M_{11}^+$               | 323                    | 320                        | 331                      | 330<br>(330)     | $M_{11}^{d+}$            | 315                    |
| $a_2$                    |                        |                            |                          |                  |                          |                        |
| $M_{12}^+$               | 988                    |                            |                          |                  | $M_{12}^{d+}$            | 802                    |
| $M_{13}^+$               | 792                    |                            |                          |                  | $M_{13}^{d+}$            | 616                    |
| $M_{14}^+$               | 346                    |                            | 396                      |                  | $M_{14}^{d+}$            | 301                    |
| $b_1$                    |                        |                            |                          |                  |                          |                        |
| $M_{15}^+$               | 998                    |                            |                          |                  | $M_{15}^{d+}$            | 840                    |
| $M_{16}^+$               | 944                    |                            |                          |                  | $M_{16}^{d+}$            | 765                    |
| $M_{17}^+$               | 758                    |                            | 791                      |                  | $M_{17}^{d+}$            | 637                    |
| $M_{18}^+$               | 587                    |                            |                          |                  | $M_{18}^{d+}$            | 328                    |
| $M_{19}^+$               | 378                    |                            |                          |                  | $M_{19}^{d+}$            | 472                    |
| $M_{20}^+$               | 131                    |                            | 126                      |                  | $M_{20}^{d+}$            | 122                    |
| $b_2$                    |                        |                            |                          |                  |                          |                        |
| $M_{21}^+$               | 3119                   |                            |                          |                  | $M_{21}^{d+}$            | 2312                   |
| $M_{22}^+$               | 3108                   |                            |                          |                  | $M_{22}^{d+}$            | 2294                   |
| $M_{23}^+$               | 1479                   |                            | 1523 <sup>g</sup>        |                  | $M_{23}^{d+}$            | 1244                   |
| $M_{24}^+$               | 1341                   |                            |                          |                  | $M_{24}^{d+}$            | 1381                   |
| $M_{25}^+$               | 1254                   |                            |                          |                  | $M_{25}^{d+}$            | 1019                   |
| $M_{26}^+$               | 1380                   |                            | 1307                     |                  | $M_{26}^{d+}$            | 1313                   |
| $M_{27}^+$               | 1129                   |                            |                          |                  | $M_{27}^{d+}$            | 827                    |
| $M_{28}^+$               | 1074                   |                            |                          |                  | $M_{28}^{d+}$            | 823                    |
| $M_{29}^+$               | 534                    | 540                        | 593                      |                  | $M_{29}^{d+}$            | 517                    |
| $M_{30}^+$               | 246                    |                            | 257                      |                  | $M_{30}^{d+}$            | 232                    |

<sup>a</sup> UB3LYP/aug-cc-pVTZ, scaled by 0.97

<sup>b</sup> Ref. 9

<sup>c</sup> Ref.20

<sup>d</sup> Ref. 18 and, in parentheses, ref. 19.

<sup>e</sup> Reassigned in the present work.

<sup>f</sup> Reassigned vibrational band.

<sup>g</sup> Assigned to a fundamental in ref. 20, but the value is far from any calculated  $b_2$  symmetry vibration here.

**Table 7.** Assignments, calculated and experimental vibrational wavenumbers ( $\text{cm}^{-1}$ ) for the  $S_0$  state of IBz- $h_5$  and IBz- $d_5$ .

| IBz- $h_5$ |                        |                      |                       | IBz- $d_5$ |                        |                         |
|------------|------------------------|----------------------|-----------------------|------------|------------------------|-------------------------|
| Mode Label | Calculated             |                      | Experimental          | Mode Label | Calculated             | Experimental            |
|            | This work <sup>a</sup> | Ref. 10 <sup>b</sup> | IR/Raman <sup>c</sup> |            | This work <sup>a</sup> | IR/Raman <sup>d</sup>   |
| $a_1$      |                        |                      |                       |            |                        |                         |
| $M_1$      | 3105                   | 3210                 | 3064                  | $M_1^d$    | 2301                   | 2290                    |
| $M_2$      | 3095                   | 3199                 | 3050                  | $M_2^d$    | 2289                   | 2273                    |
| $M_3$      | 3073                   | 3177                 | 3031                  | $M_3^d$    | 2266                   | 2270 <sup>e</sup>       |
| $M_4$      | 1562                   | 1611                 | 1575                  | $M_4^d$    | 1524                   | 1550                    |
| $M_5$      | 1461                   | 1487                 | 1473                  | $M_5^d$    | 1323                   | 1330                    |
| $M_6$      | 1046                   | 1074                 | 1060                  | $M_6^d$    | 983                    | 992                     |
| $M_7$      | 1168                   | 1194                 | 1178                  | $M_7^d$    | 855                    | 862                     |
| $M_8$      | 1004                   | 1032                 | 1015                  | $M_8^d$    | 817                    | 815 or 826 <sup>f</sup> |
| $M_9$      | 986                    | 997                  | 998                   | $M_9^d$    | 946                    | 952                     |
| $M_{10}$   | 649                    | 662                  | 654                   | $M_{10}^d$ | 622                    | 623                     |
| $M_{11}$   | 258                    | 264                  | 266                   | $M_{11}^d$ | 252                    | 256                     |
| $a_2$      |                        |                      |                       |            |                        |                         |
| $M_{12}$   | 963                    | 978                  | 963                   | $M_{12}^d$ | 785                    | 757                     |
| $M_{13}$   | 828                    | 839                  | 835                   | $M_{13}^d$ | 644                    | 680                     |
| $M_{14}$   | 398                    | 411                  | 398                   | $M_{14}^d$ | 345                    | 350                     |
| $b_1$      |                        |                      |                       |            |                        |                         |
| $M_{15}$   | 982                    | 1000                 | 987                   | $M_{15}^d$ | 816                    | 815                     |
| $M_{16}$   | 904                    | 915                  | 904                   | $M_{16}^d$ | 739                    | 735                     |
| $M_{17}$   | 728                    | 739                  | 730                   | $M_{17}^d$ | 602                    | 607                     |
| $M_{18}$   | 672                    | 699                  | 684                   | $M_{18}^d$ | 535                    | 537                     |
| $M_{19}$   | 448                    | 460                  | 448                   | $M_{19}^d$ | 396                    | 397                     |
| $M_{20}$   | 147                    | 151                  | 181                   | $M_{20}^d$ | 137                    | 158                     |
| $b_2$      |                        |                      |                       |            |                        |                         |
| $M_{21}$   | 3103                   | 3207                 | 3064                  | $M_{21}^d$ | 2296                   | 2273                    |
| $M_{22}$   | 3081                   | 3185                 | 3048                  | $M_{22}^d$ | 2275                   | 2258                    |
| $M_{23}$   | 1569                   | 1618                 | 1575                  | $M_{23}^d$ | 1533                   | 1535                    |
| $M_{24}$   | 1428                   | 1454                 | 1435                  | $M_{24}^d$ | 1298                   | 1305                    |
| $M_{25}$   | 1307                   | 1338                 | 1321                  | $M_{25}^d$ | 1267                   | 1273                    |
| $M_{26}$   | 1271                   | 1316                 | 1261                  | $M_{26}^d$ | 1016                   | 999                     |
| $M_{27}$   | 1147                   | 1173                 | 1159                  | $M_{27}^d$ | 831                    | 837                     |
| $M_{28}$   | 1063                   | 1091                 | 1068                  | $M_{28}^d$ | 811                    | 800                     |
| $M_{29}$   | 608                    | 620                  | 613                   | $M_{29}^d$ | 583                    | 587                     |
| $M_{30}$   | 212                    | 218                  | 220                   | $M_{30}^d$ | 198                    | 202                     |

<sup>a</sup> B3LYP/aug-cc-pVTZ values, scaled by 0.97

<sup>b</sup> B3LYP/aug-cc-pVDZ, unscaled.

<sup>c</sup> From ref. 6

<sup>d</sup> From ref. 21

<sup>e</sup> Estimated value from ref. 21.

<sup>f</sup> In ref. 21, a band at  $815 \text{ cm}^{-1}$  was observed in the IR spectrum, but one at  $826 \text{ cm}^{-1}$  was observed in the Raman one.



**Table 8.** Assignments, calculated and experimental vibrational wavenumbers ( $\text{cm}^{-1}$ ) for the ground state cation,  $\text{D}_0^+$ , of IBz- $h_5$  and IBz- $d_5$ .

| IBz- $h_5$ |                        |                  |                      | IBz- $d_5$    |                        |
|------------|------------------------|------------------|----------------------|---------------|------------------------|
| Mode Label | Calculated             | Experimental     |                      | Mode Label    | Calculated             |
|            | This work <sup>a</sup> | PES <sup>b</sup> | Ref. 20 <sup>c</sup> |               | This work <sup>a</sup> |
| $a_1$      |                        |                  |                      |               |                        |
| $M_1^+$    | 3119                   |                  |                      | $M_1^{d+}$    | 2314                   |
| $M_2^+$    | 3110                   |                  |                      | $M_2^{d+}$    | 2298                   |
| $M_3^+$    | 3098                   |                  |                      | $M_3^{d+}$    | 2288                   |
| $M_4^+$    | 1554                   |                  | 1575                 | $M_4^{d+}$    | 1511                   |
| $M_5^+$    | 1431                   |                  |                      | $M_5^{d+}$    | 1259                   |
| $M_6^+$    | 1007                   |                  | 1036                 | $M_6^{d+}$    | 980                    |
| $M_7^+$    | 1181                   |                  |                      | $M_7^{d+}$    | 858                    |
| $M_8^+$    | 973                    |                  | 990                  | $M_8^{d+}$    | 805                    |
| $M_9^+$    | 988                    | 1020<br>(1010)   | 1015                 | $M_9^{d+}$    | 935                    |
| $M_{10}^+$ | 651                    |                  | 661                  | $M_{10}^{d+}$ | 624                    |
| $M_{11}^+$ | 273                    | 280<br>(285)     | 284                  | $M_{11}^{d+}$ | 266                    |
| $a_2$      |                        |                  |                      |               |                        |
| $M_{12}^+$ | 986                    |                  |                      | $M_{12}^{d+}$ | 801                    |
| $M_{13}^+$ | 804                    |                  |                      | $M_{13}^{d+}$ | 625                    |
| $M_{14}^+$ | 352                    |                  | 357                  | $M_{14}^{d+}$ | 306                    |
| $b_1$      |                        |                  |                      |               |                        |
| $M_{15}^+$ | 998                    |                  |                      | $M_{15}^{d+}$ | 837                    |
| $M_{16}^+$ | 943                    |                  | 903                  | $M_{16}^{d+}$ | 760                    |
| $M_{17}^+$ | 746                    |                  | 808                  | $M_{17}^{d+}$ | 619                    |
| $M_{18}^+$ | 588                    |                  |                      | $M_{18}^{d+}$ | 477                    |
| $M_{19}^+$ | 387                    |                  | 406                  | $M_{19}^{d+}$ | 338                    |
| $M_{20}^+$ | 121                    |                  | 127                  | $M_{20}^{d+}$ | 112                    |
| $b_2$      |                        |                  |                      |               |                        |
| $M_{21}^+$ | 3117                   |                  |                      | $M_{21}^{d+}$ | 2309                   |
| $M_{22}^+$ | 3105                   |                  |                      | $M_{22}^{d+}$ | 2292                   |
| $M_{23}^+$ | 1393                   |                  |                      | $M_{23}^{d+}$ | 1253                   |
| $M_{24}^+$ | 1478                   |                  | 1517 <sup>d</sup>    | $M_{24}^{d+}$ | 1371                   |
| $M_{25}^+$ | 1333                   |                  |                      | $M_{25}^{d+}$ | 1020                   |
| $M_{26}^+$ | 1263                   |                  |                      | $M_{26}^{d+}$ | 1335                   |
| $M_{27}^+$ | 1140                   |                  |                      | $M_{27}^{d+}$ | 831                    |
| $M_{28}^+$ | 1077                   |                  |                      | $M_{28}^{d+}$ | 825                    |
| $M_{29}^+$ | 554                    |                  | 538                  | $M_{29}^{d+}$ | 535                    |
| $M_{30}^+$ | 216                    |                  | 242                  | $M_{30}^{d+}$ | 203                    |

<sup>a</sup> UB3LYP/aug-cc-pVTZ, scaled by 0.97

<sup>b</sup> Conventional photoelectron study: ref. 22 and, in parentheses, ref. 19.

<sup>c</sup> One-photon MATI study.

<sup>d</sup> Assigned to a fundamental in ref. 20, but the value is far from any calculated  $b_2$  symmetry vibration here.

## Figure Captions

**Figure 1.** Complete 0–3050  $\text{cm}^{-1}$  spectral range scan of the  $S_1 \leftarrow S_0$  (1+1) REMPI spectra of BrBz- $h_5$  (top trace, upright) and BrBz- $d_5$  (bottom trace, inverted).

(The final vibrational level is given with all transitions emanating from the ground state zero point vibrational level;  $M_i^n$  represents a transition to  $n$  quanta of the  $M_i$  vibration.) The assignments are discussed in the text: in detail for the region  $< 1050 \text{ cm}^{-1}$ , and in more general terms for the higher wavenumber features. The “combs” indicate regions of the spectrum whose contributors also appear to higher wavenumber in combination with another vibration, although the precise assignment of the individual features is not necessarily clear.

**Figure 2.** Generalized Duschinsky matrix between vibrational modes of the  $S_0$  states of FBz- $h_5$  and BrBz- $h_5$ . Shadings indicate the mixing coefficient values, with black = 1.00 while white = 0.00, with the level of the grey shading indicating intermediate values. The numbers are the  $i$  values for each  $M_i$  mode.

**Figure 3.** Generalized Duschinsky matrix between the vibrational modes of the  $S_0$  states of BrBz- $h_5$  and BrBz- $d_5$ . Shadings indicate the mixing coefficient values, with black = 1.00 while white = 0.00, with the level of the grey shading indicating intermediate values. The numbers are the  $i$  values for each  $M_i$  or  $M_i^d$  mode. See text for details. Note that the  $M_6^d$  and  $M_8^d$  modes mix significantly, with the Duschinsky approach suggesting an incorrect dominant contribution in each case; however, the identification of the modes is clear from the form of the modes, and the spectrum – see text.

**Figure 4.** Generalized Duschinsky matrices between the vibrational modes of the  $S_0$  and  $S_1$  states for: (a) BrBz- $h_5$  and (b) BrBz- $d_5$ . Shadings indicate the mixing coefficient values, with black = 1.00 while white = 0.00, with the level of the grey shading indicating intermediate values. The numbers are the  $i$  values for each  $M_i$  or  $M_i^d$  mode. See text for details.

**Figure 5.** Expanded views of the low wavenumber regions (0–750  $\text{cm}^{-1}$ ) of the  $S_1 \leftarrow S_0$  (1+1) REMPI spectra of BrBz- $h_5$  (top trace, upright) and BrBz- $d_5$  (bottom trace, inverted). Assignments are discussed in the text and summarized in Tables 4 and 5; suggested assignments for some of the weaker features and the region marked  $\alpha$  are also given in these tables. (The final vibrational level is given with all transitions emanating from the ground state zero point vibrational level;  $M_i^n$  represents a transition to  $n$  quanta of the  $M_i$  vibration.)

**Figure 6.** Expanded views of the medium wavenumber regions (750–1050  $\text{cm}^{-1}$ ) of the  $S_1 \leftarrow S_0$  (1+1) REMPI spectra of BrBz- $h_5$  (top trace, upright) and BrBz- $d_5$  (bottom trace, inverted). Assignments are discussed in the text and summarized in Tables 4 and 5; suggested assignments for some of the weaker features and the region marked  $\beta$  are also given in these tables. (The final vibrational level is given with all transitions emanating from the ground state zero point vibrational level;  $M_i^n$  represents a transition to  $n$  quanta of the  $M_i$  vibration.)

**Figure 7.** Generalized Duschinsky matrices between the vibrational modes of: (a) the  $S_0$  and  $D_0^+$  states for BrBz- $h_5$  and (b) the  $S_1$  and the  $D_0^+$  states for BrBz- $h_5$ . Shadings indicate the normalized coefficient values, with black = 1.00 while white = 0.00, with the level of the grey shading indicating intermediate values. The numbers are the  $i$  values for each  $M_i/M_i^+$  mode. See text for details.

**Figure 8.** Generalized Duschinsky matrices between the vibrational modes of: (a) the  $S_0$  for IBz- $h_5$  and  $S_0$  IBz- $d_5$  and (b) the  $S_0$  and the  $D_0^+$  states for IBz- $h_5$ . Shadings indicate the normalized coefficient values, with black = 1.00 while white = 0.00, with the level of the grey shading indicating intermediate values. The numbers are the  $i$  values for each  $M_i/M_i^d/M_i^+$  mode. As can be seen from (a), the  $M_6^d$  and  $M_8^d$  modes mix significantly, with the Duschinsky approach suggesting an incorrect dominant contribution in each case; however, the identification of the modes is clear from the form of the modes, and by comparison with BrBz- $d_5$  – see text.

Figure 1.

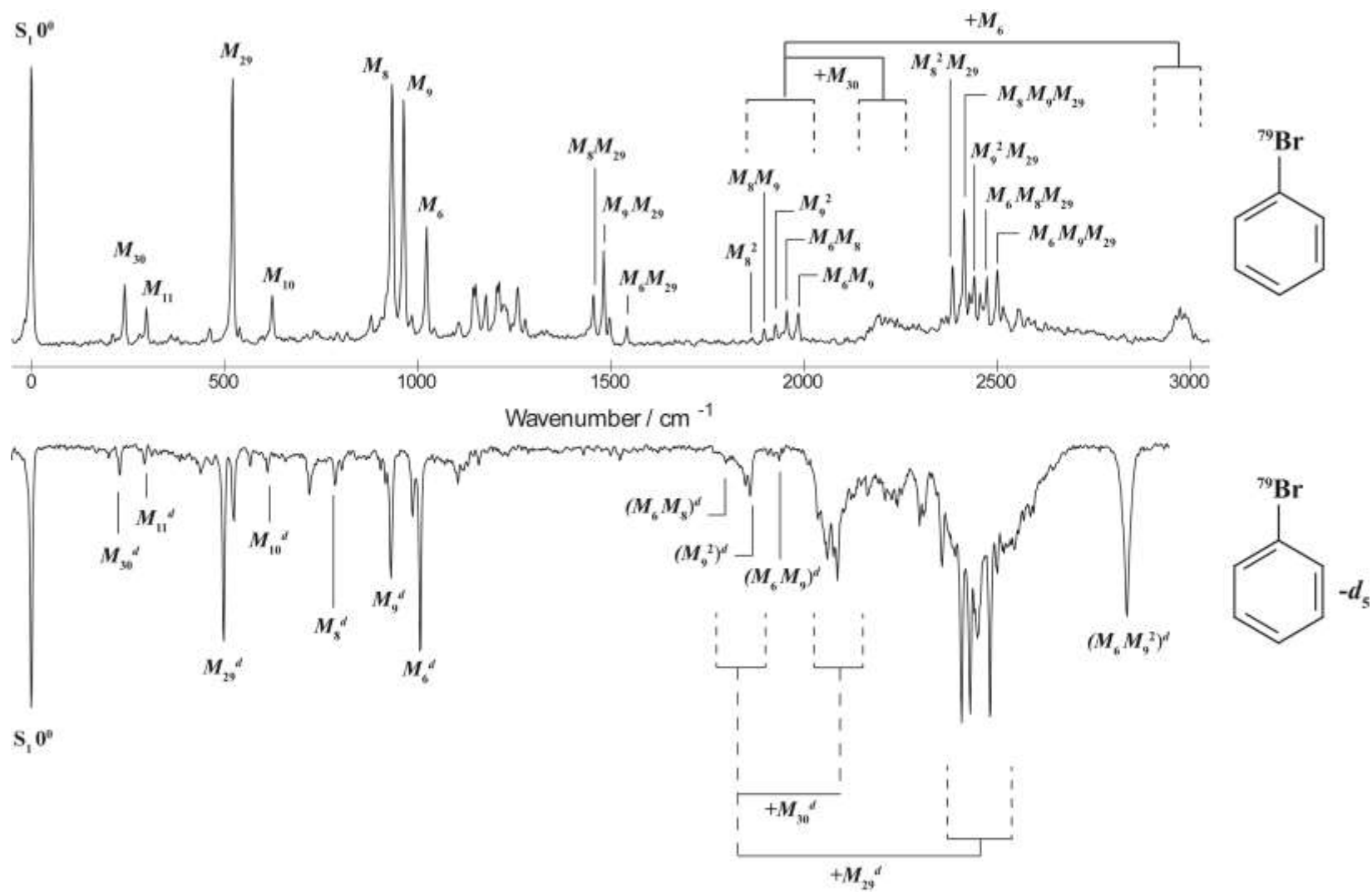


Figure 2.

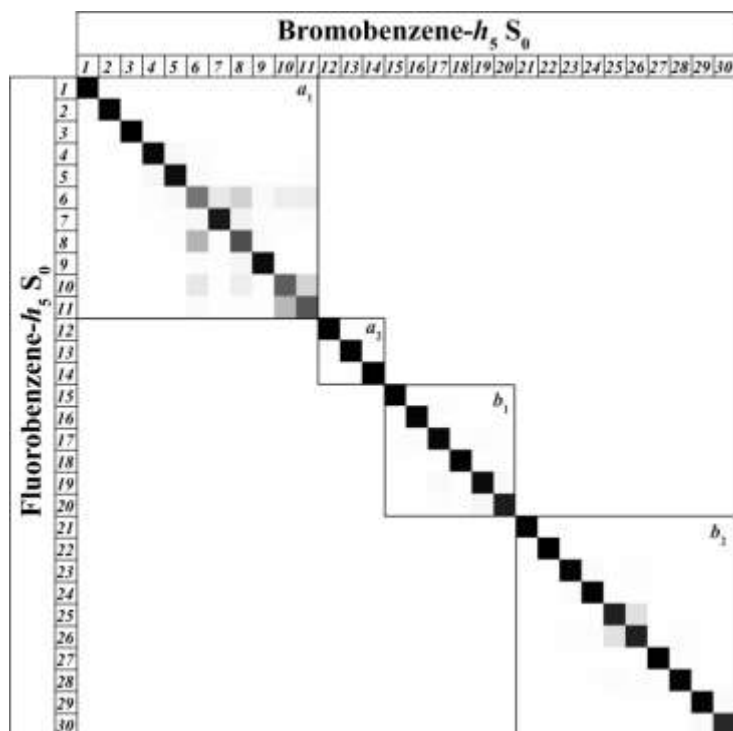


Figure 3.

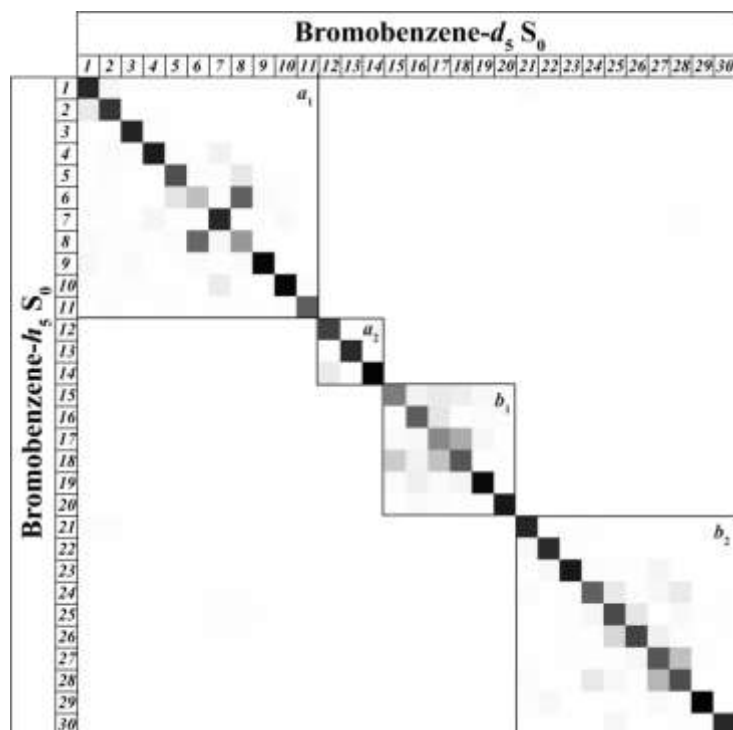


Figure 4.

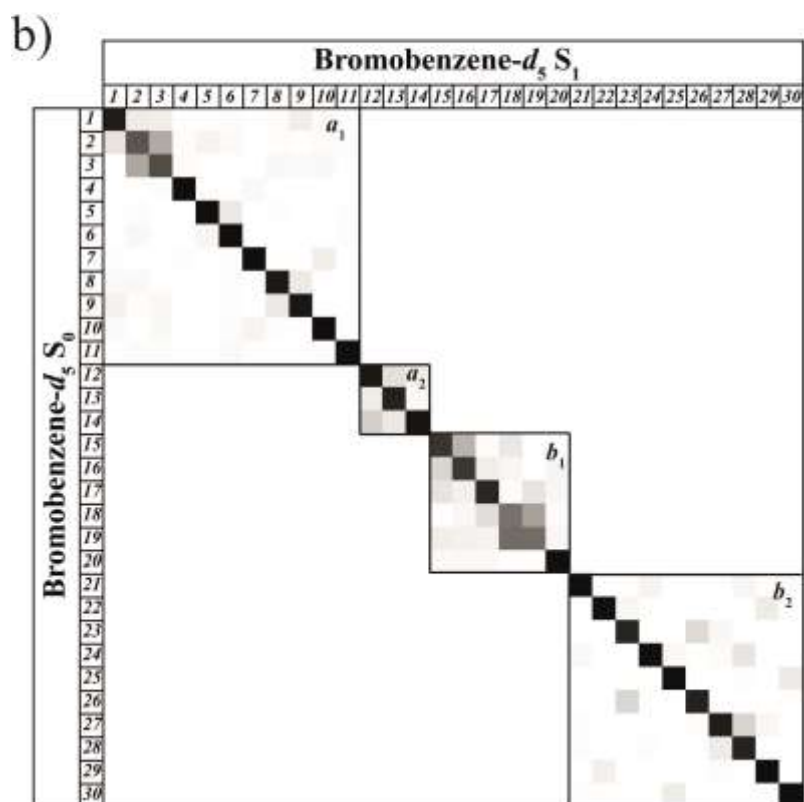
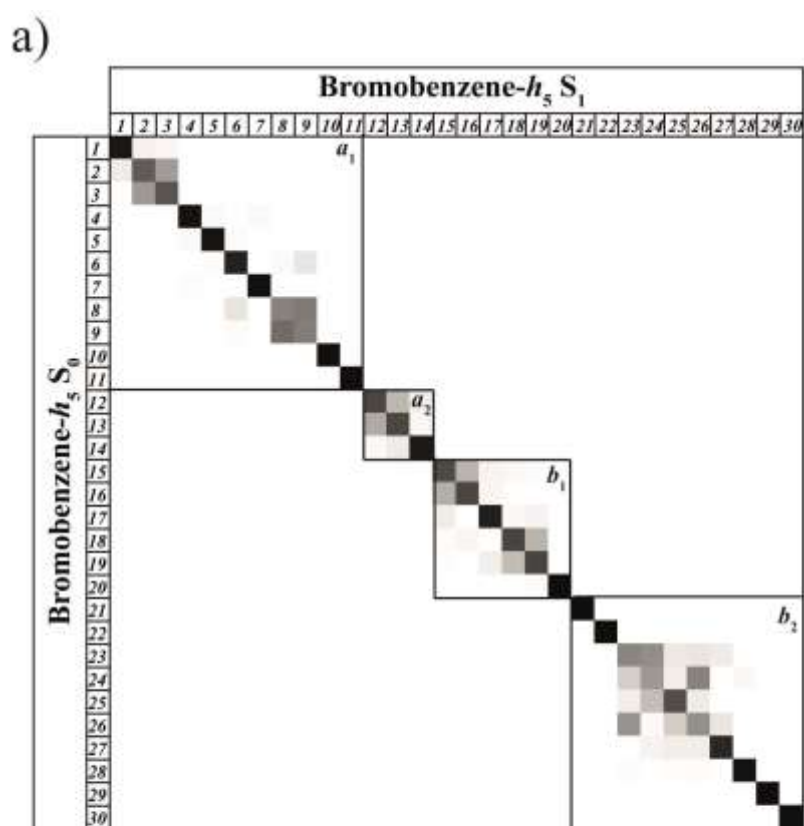


Figure 5.

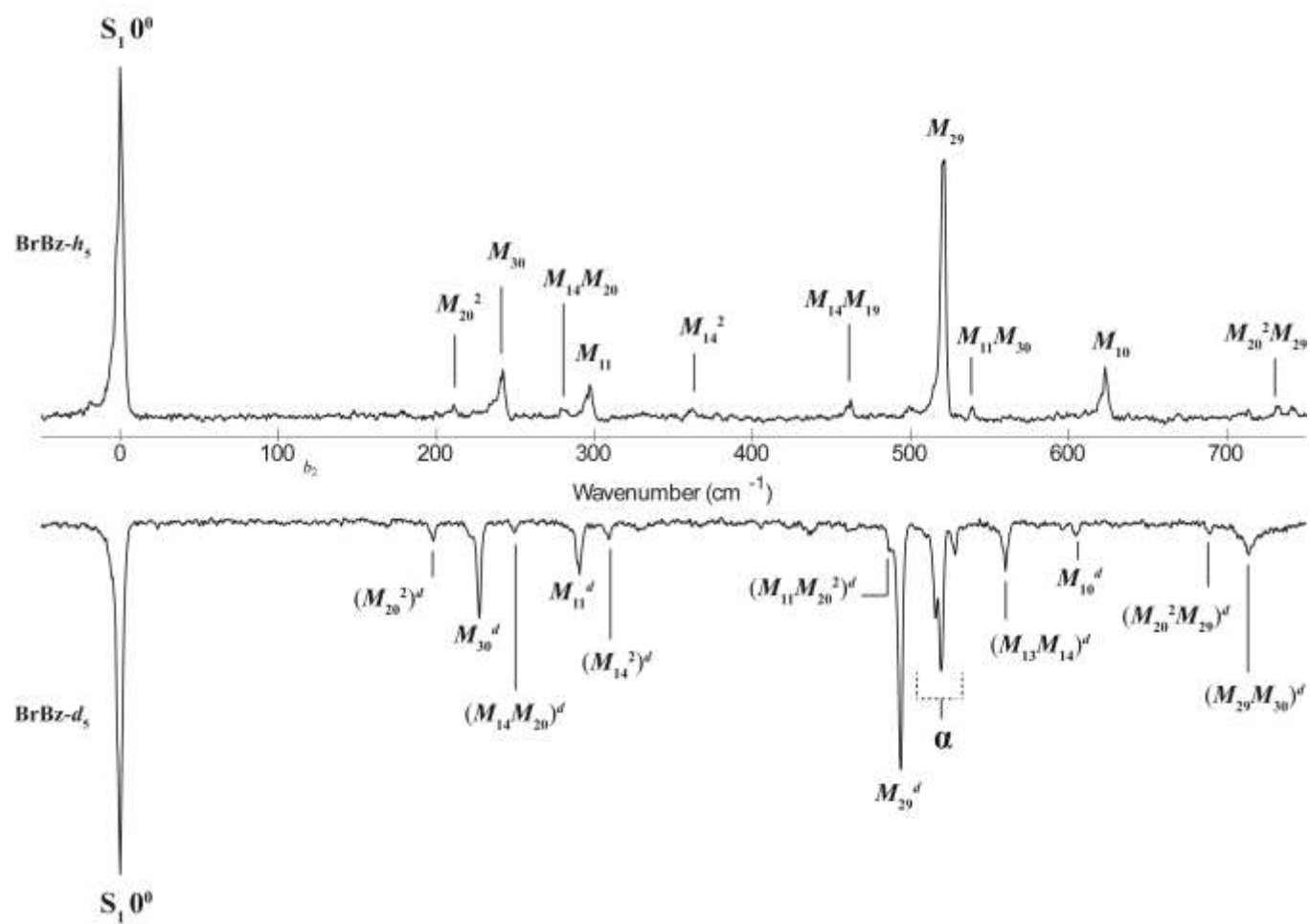


Figure 6.

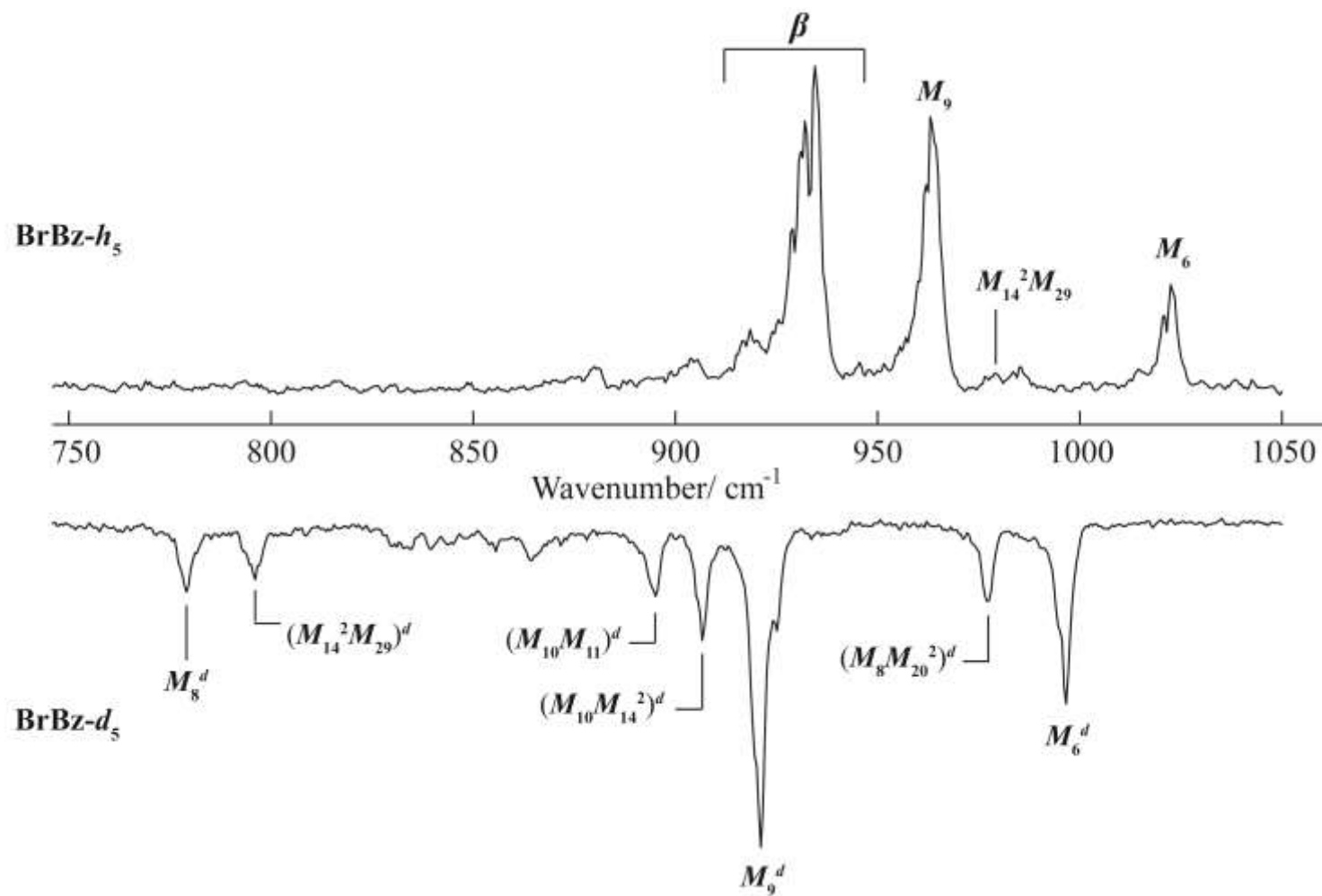




Figure 7.

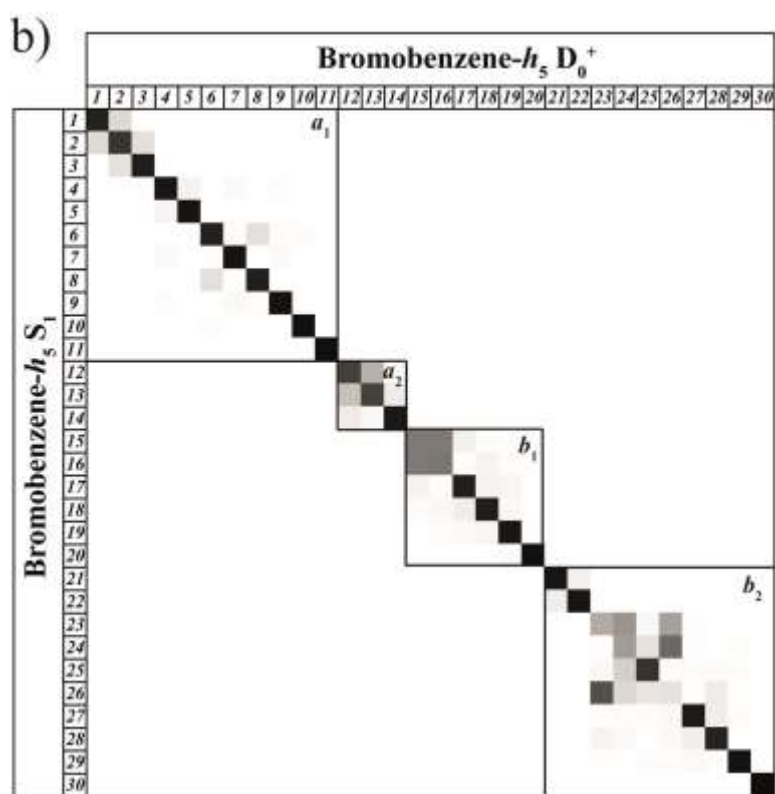
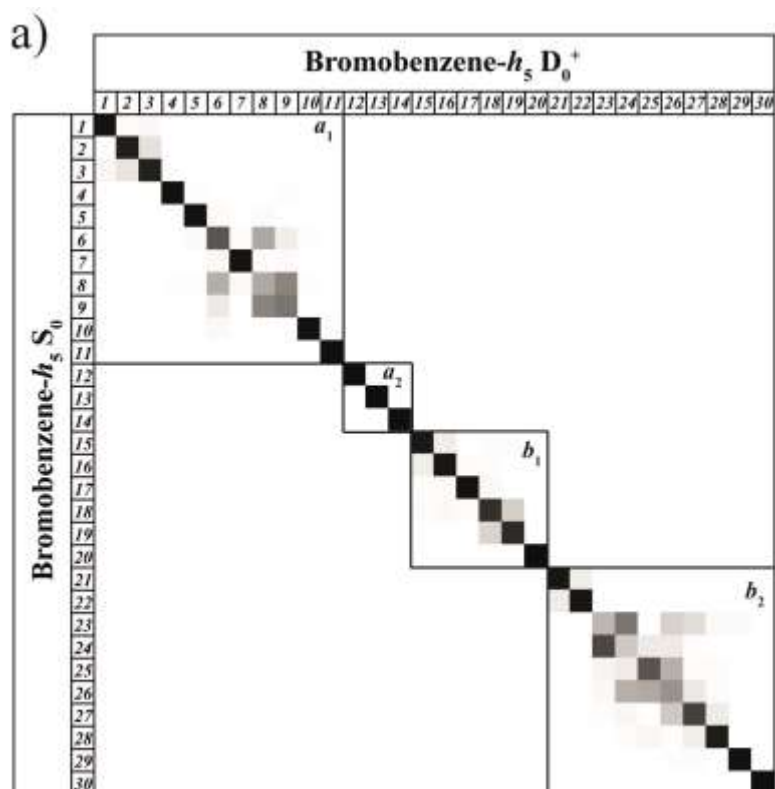
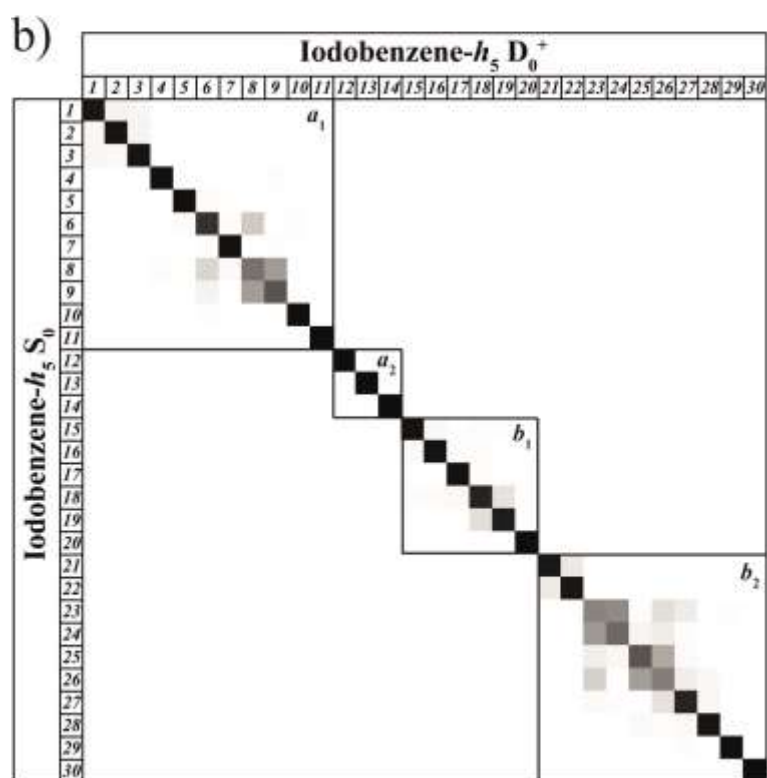
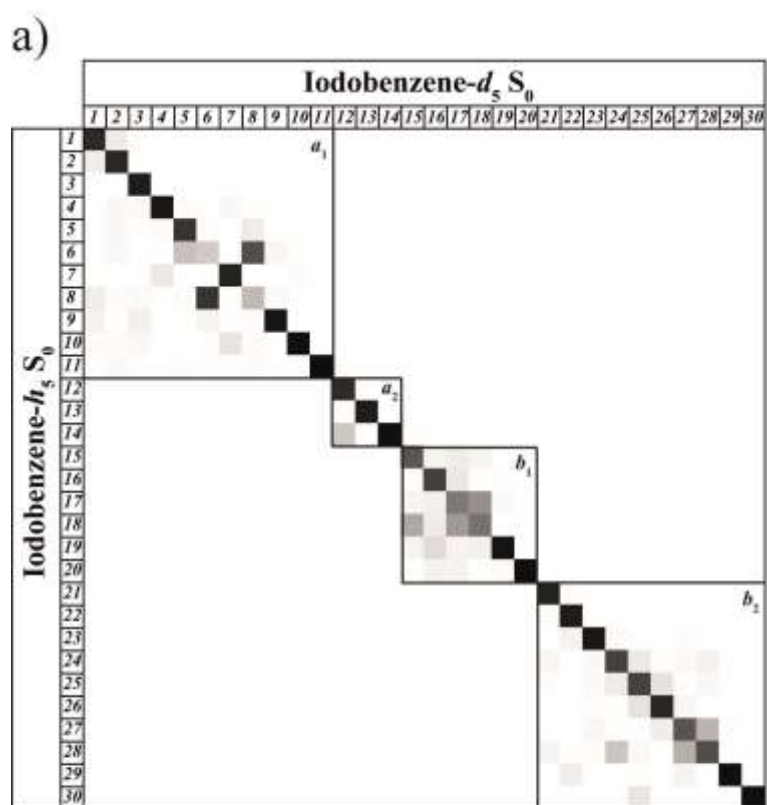


Figure 8.



## References

---

- <sup>1</sup> J. P. Harris, A. Andrejeva, W. D. Tuttle, I. Pugliesi, C. Schrieffer, and T. G. Wright, *J. Chem. Phys.*, **141**, 244315 (2014)
- <sup>2</sup> A. Andrejeva, W. D. Tuttle, J. P. Harris and T. G. Wright, accepted for publication by *J. Chem. Phys.*
- <sup>3</sup> K. W. K. Kohlrausch and H. Wittek, *Monatsh. Chem.* **74**, 1 (1941).
- <sup>4</sup> E. K. Plyler, *Disc. Faraday Soc.* **9**, 100 (1950).
- <sup>5</sup> G. Varsányi, *Assignments of the Vibrational Spectra of Seven Hundred Benzene Derivatives* (Wiley, New York, 1974)
- <sup>6</sup> D. H. Whiffen, *J. Chem. Soc.* 1350 (1950).
- <sup>7</sup> P. R. Griffiths and H. W. Thompson, *Proc. R. Soc. London* **298**, 51 (1967).
- <sup>8</sup> E. B. Wilson, Jr, *Phys. Rev.*, **45**, 706 (1934)
- <sup>9</sup> K. Walter, K. Scherm and U. Boesl, *J. Phys. Chem.*, **95**, 1188 (1991)
- <sup>10</sup> A. M. Gardner and T. G. Wright. *J. Chem. Phys.* **135**, 114305 (2011).
- <sup>11</sup> R. S. Mulliken, *J. Chem. Phys.*, **23**, 1997 (1955)
- <sup>12</sup> I. Walerstein, *Phys. Rev* **59**, 924 (1941).
- <sup>13</sup> K. Sreeramamurty, *Curr. Sci.* **18**, 437 (1949).
- <sup>14</sup> S. Prakash and N. L. Singh, *J. Sci. Ind. Res. B* **21**, 512 (1962).
- <sup>15</sup> G. V. Klimusheva, L. S. Kostyuschenko, L. M. Sverdlov, and G. M. Suroka, *Opt. Spectrosc. (USSR)* **40**, 141 (1976) [*Opt. Spectrosk.* **40**, 245 (1971)].
- <sup>16</sup> T. G. Dietz, M. A. Duncan, M. G. Liverman and R. E. Smalley, *J. Chem. Phys.*, **73**, 4816 (1980)
- <sup>17</sup> U. Boesl, R. Zimmermann, C. Weickhardt, D. Lenoir, K.-W. Schramm, A. Kettrup and E. W. Schlag, *Chemosphere*, **29**, 1229 (1994).
- <sup>18</sup> D. M. P. Holland, D. Edvardsson, L. Karlsson, R. Maripuu, K. Siegbahn, A. W. Potts and W. von Niessen, *Chem. Phys.*, **252**, 257 (2000)
- <sup>19</sup> A. W. Potts, M. L. Lyus, E. P. F. Lee, and G. H. Fattahallah, *J. Chem. Soc., Farad. Trans. 2*, **76**, 556 (1980).
- <sup>20</sup> C. H. Kwon, H. L. Kim and M. S. Kim, *J. Chem. Phys.*, **116**, 10361 (2002)
- <sup>21</sup> T. R. Nanney, E. R. Lippincott and J. C. Hamer, *Spectrochimica Acta*, **23**, 737 (1966)
- <sup>22</sup> D.M.P Holland, D Edvardsson, L Karlsson, R Maripuu, K Siegbahn, A.W Potts, W.von Niessen, *Chem. Phys.*, **253**, 133 (2000).
- <sup>23</sup> *Gaussian 09*, Revision C.01, M. J. Frisch, G. W. Trucks, H. B. Schlegel, G. E. Scuseria, M. A. Robb, J. R. Cheeseman, G. Scalmani, V. Barone, B. Mennucci, G. A. Petersson, H. Nakatsuji, M. Caricato, X. Li, H. P. Hratchian, A. F. Izmaylov, J. Bloino, G. Zheng, J. L. Sonnenberg, M. Hada, M. Ehara, K. Toyota, R. Fukuda, J. Hasegawa, M. Ishida, T. Nakajima, Y. Honda, O. Kitao, H. Nakai, T. Vreven, J. A. Montgomery, Jr., J. E. Peralta, F. Ogliaro, M. Bearpark, J. J. Heyd, E. Brothers, K. N.

- 
- Kudin, V. N. Staroverov, R. Kobayashi, J. Normand, K. Raghavachari, A. Rendell, J. C. Burant, S. S. Iyengar, J. Tomasi, M. Cossi, N. Rega, J. M. Millam, M. Klene, J. E. Knox, J. B. Cross, V. Bakken, C. Adamo, J. Jaramillo, R. Gomperts, R. E. Stratmann, O. Yazyev, A. J. Austin, R. Cammi, C. Pomelli, J. W. Ochterski, R. L. Martin, K. Morokuma, V. G. Zakrzewski, G. A. Voth, P. Salvador, J. J. Dannenberg, S. Dapprich, A. D. Daniels, Ö. Farkas, J. B. Foresman, J. V. Ortiz, J. Cioslowski, and D. J. Fox, Gaussian, Inc., Wallingford CT, 2009.
- <sup>24</sup> I. Pugliesi and K. Muller-Dethlefs, *J. Phys. Chem. A*, **110**, 4657 (2006), a free download of the software can be found at <http://www.fclab2.net>
- <sup>25</sup> PGOPHER, a Program for Simulating Rotational, Vibrational and Electronic Structure, C. M. Western, University of Bristol, <http://pgopher.chm.bris.ac.uk>. PGOPHER version 8.0, C M Western, 2014, University of Bristol Research Data Repository, doi:10.5523/bris.huflggvpcuc1zvliqed497r2.
- <sup>26</sup> T. Cvitas, *Mol. Phys.*, **19**, 297 (1970)
- <sup>27</sup> A. de la Cruz, J. Campos and M. Ortiz, *J. Mol. Spec.*, **180**, 305 (1996)
- <sup>28</sup> See supplemental material at [URL will be inserted by AIP] for tables of calculated vibrational wavenumbers of the <sup>81</sup>BrBz-*h*<sub>5</sub> and <sup>81</sup>BrBz-*d*<sub>5</sub> isotopologues compared to the corresponding <sup>79</sup>BrBz ones.
- <sup>29</sup> A. M. Gardner, A. M. Green, V. M. Tamé-Reyes, K. L. Reid, J. A. Davies, V. H. K. Parkes, and T. G. Wright, *J. Chem. Phys.* **140**, 114308 (2014).
- <sup>30</sup> See, for example, Y.-J. Liu, P. Persson, and S. Lunell, *J. Phys. Chem. A* **108**, 2339 (2004).
- <sup>31</sup> A. G. Sage, T. A. A. Oliver, D. Murdock, M. B. Crow, G. A. D. Ritchie, J. N. Harvey, and M. N. R. Ashfold, *Phys. Chem. Chem. Phys.* **13**, 8075 (2011).